New Accurate Ideas on Flavor Formation in Hadronization and Connections to QCD

C.D. Buchanan and Sebong Chun
UCLA, Los Angeles, CA 90024

Presented by C.D. Buchanan

April 2, 1997

Abstract

Our work strongly suggests a paradigm shift in understanding flavor creation within relativistic string approaches, a paradigm shift to a viewpoint in which suppression of heavy particle formation (kaon, η, ρ, ϕ, proton, Λ, etc) predominantly comes directly from the final state hadronic mass, not from the virtual $q\bar{q}$ production level (s/u, qq/q,...) nor from the hadronic formation level (vector/all,...). Our predictions are especially clean and accurate for the production of various flavored mesons, the most fundamental and elementary tests of colorfield behavior. Our approach also forms an excellent 'platform' for future understanding of baryon formation, P_T effects, etc. The central feature of our approach is a simple *Event Weight Function* which, on the one hand, leads with very few assumptions to predictions agreeing quite well with e^+e^- hadronization data and, on the other hand, connects persuasively to strong-coupled soft non-perturbative QCD and forms a 'target' for calculations within this regime.

1 Introduction

It is commonly believed that QCD may well be the appropriate underlying theory for the 'hadronization process' (how hadrons are produced).

Hadronization can occur in many different arenas: hadron-hadron interactions, lepton-hadron interactions, etc. The cleanest arena in which to study it is electron-positron interactions in which the electro-weak annihilation creates an almost asymptotically free initial quark-antiquark pair at very large Q^2, with a QCD colorfield emerging between the pair as they separate. The system then evolves from its initial condition, in which perturbative QCD can be used to calculate intermediate-state gluon emission, into a very soft low-Q^2 non-perturbative regime in which the hadrons are finally created. The most fundamental and elementary testing ground for hadronization ideas is meson formation and distributions.

The conceptual path from QCD to accurate predictions of e^+e^- data is sketched in Fig.1.

The central feature for our UCLA approach is an *Event Weight Function* (dW_f) which can be written for any final state of specified hadrons - that is, where the flavor (and, therefore, mass) and 3-momentum of each hadron is specified - and which provides the probability of that specific event occurring relative to other possible final states. The nomenaclature of such an event is shown in Fig.2.

In our present view, we now conceptualize the path as moving logically from QCD to dW_f to dP_1 (the fragmentation function for an 'outside-in, one-hadron-at-a-time' implementation) to comparisons with data (See Fig.1). However, historically, quite the reverse is true: We first noted in 1987[1] that if the Lund Symmetric Fragmentation Function[2, 3]

$$f(z, P_{T_h}^2) = N \, \frac{(1-z)^a}{z} \, e^{-b \, \left(m_h^2 + P_{T_h}^2\right)/z} \tag{1}$$

was used as a hadronic production density (i.e., with constant normalization N for all hadrons), then the predicted rates agreed rather well with measured ones. In this approach the suppression of heavy hadrons arose from the $\exp(-bm_H^2/z)$ factor rather than from suppression factors such as s/u and Vector/All as used, for example, in the Lund implementation. After this initial phenomenological success, we then began, with some guidance from the Lund group, to develop the idea and form of the *Event Weight Function*[4] which not only leads to the idea of using the Lund Symmetric Fragmentation Function with constant normalization, but also begins to connect with QCD for which it potentially forms a 'target' for approximate calculations, lattice work, etc.

The Path From QCD to Hadronization DATA
(via The UCLA Approach)

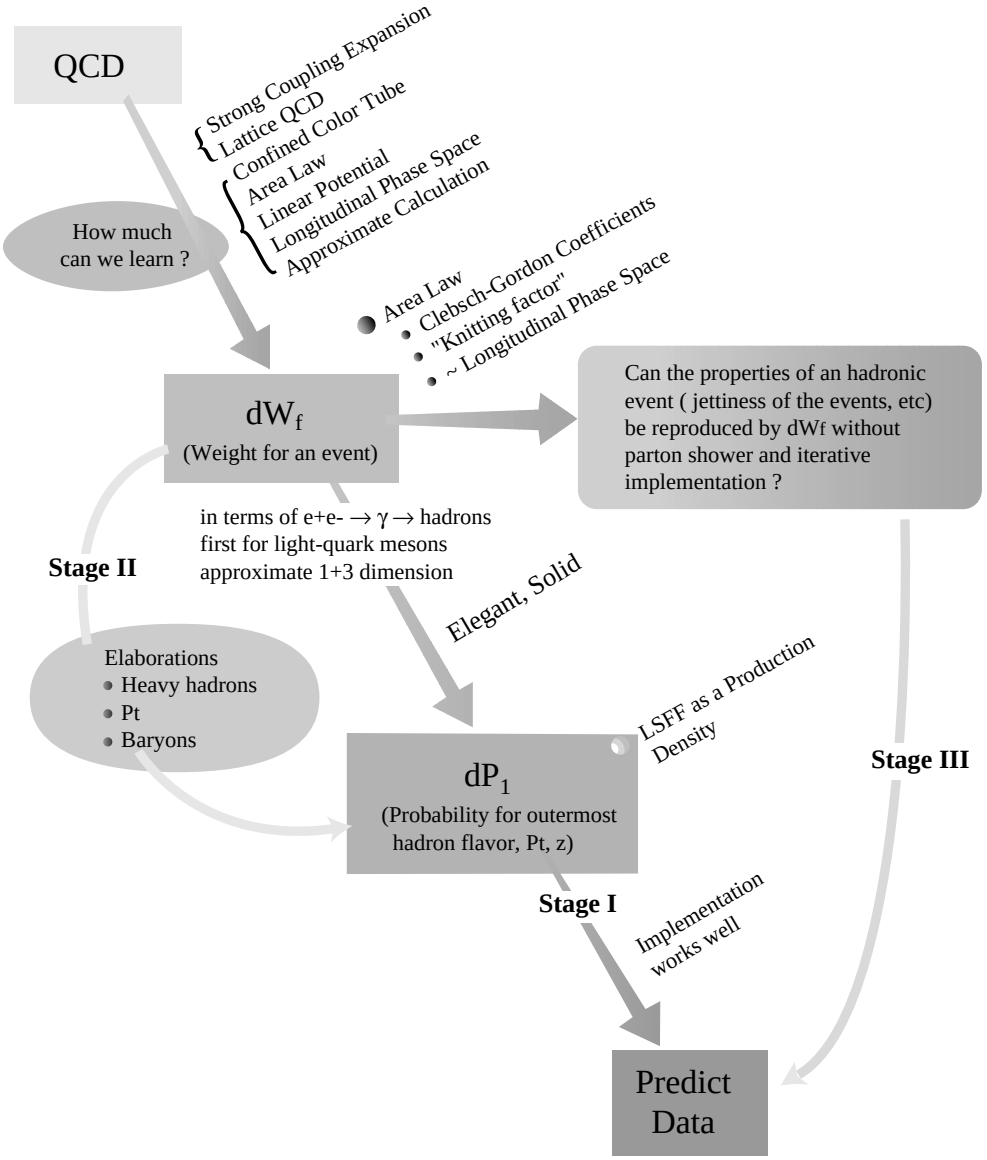

Figure 1: The conceptual flow of the UCLA approach from QCD to the *Event Weight Function* to the *Fragmentation Function* to predictions of data. [Note, however, that the historical development proceeded in roughly the opposite sequence.]

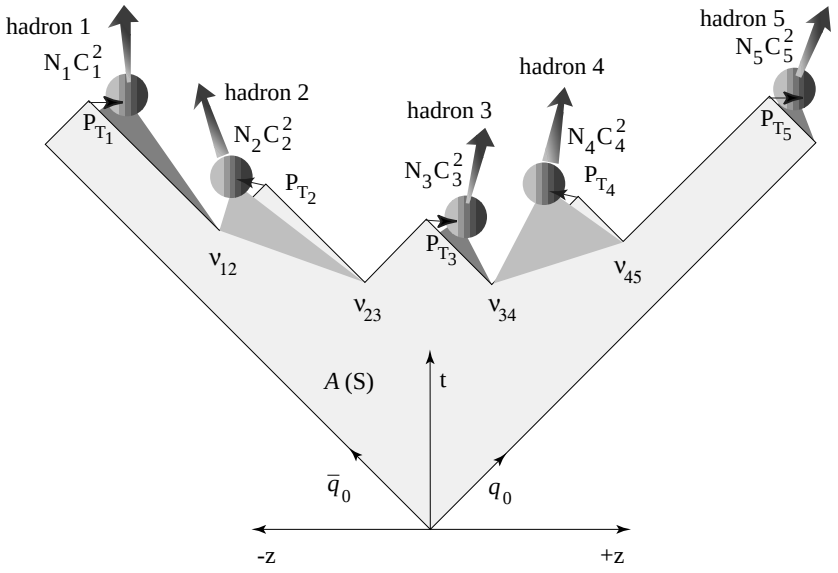

Figure 2: Five hadrons are produced with small intrinsic P_T relative to a *"planar"* hadronic event of e^+e^- annihilation. These P_T's distort the plane of the event in such a way that the resulting area becomes slightly larger than for the planar event. See text for description of ν_{ij}, C_i^2, N_i, and of our UCLA assumptions for these.

The *Event Weight Function* involves very simple principles: An area law[5] in space-time (which almost any strong-coupled theory will suggest), approximately longitudinal phasespace, the possibility of suppression 'penalties' in creating massive quark-antiquark pairs from the colorfield (ν_{ij} in Fig.2), Clebsch-Gordon coefficients to describe the flavor and spin combination of a quark and antiquark as they coalesce into a meson or of three quarks into a baryon (C_i^2), and 'knitting factors' to describe the combinations into the spatial wave functions of the hadron to be created (N_i). In our UCLA modeling we make the simplest possible assumptions within this structure:

i) that there is no appreciable suppression for creating light-quark pairs from the colorfield [namely, $\nu_{ij} \simeq 1.0$ for $u\bar{u}$, $d\bar{d}$, and $s\bar{s}$ virtual pairs from the colorfield] and

ii) that the spatial 'knitting factors' for forming all hadrons are approximately the same (namely, all $N_i \simeq (75MeV)^{-2} = (2.7fm)^2$).

How should we go about testing our *Event Weight Function* hypothesis against experimental data? The ideal way would be to have a computer big enough and fast enough that, for a given E_{CM}, a library of *Event Weight Functions* could be calculated for each possible set of final state hadrons within a grid of the flavor (mass), longitudinal momentum and transverse momentum of each hadron produced. This, unfortunately, is not practical, but it is useful to remind the reader that the goal is a method to simulate this ideal. The practical technique to carry this out is to use a Monte Carlo program in which one hadron at a time is picked in such a way that an event as-a-whole is eventually constructed appropriately.

The program we use is an adaptation of the relativistic string Monte Carlo JETSET7.4[6] written by Dr.Torbjorn Sjöstrand of Lund University, Sweden (with many thanks to him for making it available to us and aiding us in using it). The program uses an 'outside-in' implementation, that is, first picking the outermost hadron containing the initial quark, and then working its way inward.

Thus it is necessary for us, beginning with a *Event Weight Function* for an event, to derive the fragmentation function - i.e., the probability (dP_1) - for the flavor and momentum of a first outermost hadron. (See, e.g., Fig.2.) When we perform this derivation, we find that our simple UCLA assumptions for the *Event Weight Function* vertex suppression and knitting factors yield

essentially the phenomenology which we originally found to be successful: namely, using the Lund Symmetric Fragmentation Function as a hadronic production density in the outside-in JETSET implementation framework!

2 The Event Weight Function dW_f for Meson Formation

Referring to Fig.2, the Event Weight Function for an event with a final state f is written as:

$$
\begin{aligned}
dW_f{}^{q_0\bar{q}_0} &= \frac{N_1 C_1^2}{(2\pi)^3} dE_1 dP_{z_1} dP_{x_1} dP_{y_1} \delta\left(E_1^2 - P_1^2 - m_1^2\right) \nu_{12} \times \ldots \\
&\times \frac{N_{n-1} C_{n-1}^2}{(2\pi)^3} dE_{n-1} dP_{z_{n-1}} dP_{x_{n-1}} dP_{y_{n-1}} \delta\left(E_{n-1}^2 - P_{n-1}^2 - m_{n-1}^2\right) \nu_{n-1,n} \\
&\times \frac{N_n C_n^2}{(2\pi)^3} dE_n dP_{z_n} dP_{x_n} dP_{y_n} \delta\left(E_n^2 - P_n^2 - m_n^2\right) \\
&\times (2\pi)^4 \delta\left(\mathbf{E} - \sum_i E_i\right) \delta\left(\mathbf{P}_z - \sum_i P_{z_i}\right) \delta\left(\mathbf{P}_x - \sum_i P_{x_i}\right) \delta\left(\mathbf{P}_y - \sum_i P_{y_i}\right) \\
&\times e^{-b' \mathcal{A}_{\mathrm{world-surface}}}
\end{aligned}
\tag{2}
$$

where

$$
\left(\frac{1}{2\pi}\right)^3 dE_i dP_{z_i} dP_{x_i} dP_{y_i} \delta\left(E_i^2 - P_{z_i}^2 - P_{x_i}^2 - P_{y_i}^2 - m_i^2\right) \tag{3}
$$

is just the four-dimensional phasespace

$$
\left(\frac{1}{2\pi}\right)^3 d^4P \delta\left(P_i^2 - m_i^2\right) = \left(\frac{1}{2\pi}\right)^3 \frac{d^3P_i}{2E_i}
$$

for the i-th meson and

$$
(2\pi)^4 \delta\left(\mathbf{E} - \sum_i E_i\right) \delta\left(\mathbf{P}_z - \sum_i P_{z_i}\right) \delta\left(\mathbf{P}_x - \sum_i P_{x_i}\right) \delta\left(\mathbf{P}_y - \sum_i P_{y_i}\right) \tag{4}
$$

is overall four-momentum conservation. The bold face $\mathbf{E}$ signifies E^{total}, etc. The factor $\exp(-b'\mathcal{A}_{\mathrm{world-surface}})$ is the QCD-inspired space-time area law factor and the ν_{ij}'s are the vertex suppression factors possible at the production of each virtual $q\bar{q}$ pair from the colorfield.

We include a structure to describe the probability that a quark from one virtual vertex and an anti-quark from an adjacent vertex combine to form the state function of a final meson. This involves both Clebsch-Gordon coefficients to control the flavor and spin parts (the C_i^2s) and a 'knitting factor' N_i for the spatial part of the hadrons state function.

The factor $\exp(-b'\mathcal{A}_{\text{world-surface}})$ is the area law behavior which, as will be discussed in Section 7, most approaches to strong-coupling situations (such as that of hadronization in its later stages) lead to, where b' is a parameter which is related to the string constant and $\mathcal{A}$ is the area swept out in a space-time diagram such as Fig.2. Because the JETSET implementation provides a good recipe for iterating past a gluon-induced string kink, eq(2) is rewritten relative to a straight relativistic string using

$$\mathcal{A}_{\text{world-surface}} \simeq \mathcal{A}_{plane} + \sum_i \frac{\chi_i}{b'} P_{T_i}^2$$

where $\mathcal{A}_{plane}$ is the area of world-surface projected to a plane. This yields

$$\begin{aligned} dW_f{}^{q_0\bar{q}_0} &= \frac{N_1 C_1^2}{(2\pi)^3} dE_1 dP_{z_1} dP_{x_1} dP_{y_1} \delta\left(E_1^2 - P_1^2 - m_1^2\right) e^{-\chi\left(P_{x_1}^2 + P_{y_1}^2\right)} \nu_{12} \times \ldots \\ &\times \nu_{n-1,n} \frac{N_n C_n^2}{(2\pi)^3} dE_n dP_{z_n} dP_{x_n} dP_{y_n} \delta\left(E_n^2 - P_n^2 - m_n^2\right) e^{-\chi\left(P_{x_n}^2 + P_{y_n}^2\right)} \\ &\times (2\pi)^4 \delta\left(\mathbf{E} - \sum_i E_i\right) \delta\left(\mathbf{P}_z - \sum_i P_{z_i}\right) \delta\left(\mathbf{P}_x - \sum_i P_{x_i}\right) \delta\left(\mathbf{P}_y - \sum_i P_{y_i}\right) \\ &\times e^{-b'\mathcal{A}_{plane}} \end{aligned} \tag{5}$$

This *Event Weight Function* structure can be used to analyze both the Lund and the UCLA approaches to the situation.

The UCLA assumptions are:

i) The ν_{ij}s for $u\bar{u}$, $d\bar{d}$, and $s\bar{s}$ are all ≈ 1.0, that is, there is no substantial penalty for creating any $q\bar{q}$ pair, at least as long as the quark mass is below the QCD scale of $\approx 1GeV$. This also recognizes that at this stage the event is very close (in time or virtuality) to the actual final state hadrons and that the virtual quark pair production from the colorfield is being 'pulled' by the configurations of allowable final state hadrons.

ii) The Clebsch-Gordon coefficients for creating mesons are remarkably simple, flowing from three aspects of our approach:

(a) Only sets of final state hadrons are allowed which correspond to local flavor conservation in creating virtual pairs in the colorfield. That is, virtual $u\bar{u}$, $d\bar{d}$, and $s\bar{s}$ pairs can be created locally in the colorfield, but $u\bar{d}$, $u\bar{s}$, and $d\bar{s}$ pairs cannot.

(b) If, for example, a k^+ meson is part of a hypothesized *local-flavor-conservation-allowed chain*, then the $u\bar{s}$ pair needed to form the k^+ is simply available. The flavor coupling, then, of this 'available' $u\bar{s}$ pair into the k^+ flavor state function, whose only flavor composition is $u\bar{s}$, is simply 1.0. Note, however, for example, that a π^0 has equal terms in both $u\bar{u}$ and $d\bar{d}$ composition. Thus, if a $u\bar{u}$ mesonic combination is allowed by a hypothesized local-flavor-conservation chain, then this $u\bar{u}$'s coupling to the π^0's flavor state function would be 0.5. Similarly, the couplings which we use into either an η or into an η' have strength 0.25 from $u\bar{u}$, 0.25 from $d\bar{d}$, and 0.5 from $s\bar{s}$.

(c) The spins of the final state hadrons are presumed to be (at least, approximately) independent. Given the intense amount of spin angular momentum in the gluons of the colorfield, this would seem to be a plausible approximate assumption. Therefore, the colorfield couples in spin to a final state hadron simply with the hadron's spin degrees of freedom.

Thus, to summarize, the colorfield couples to a final state meson in flavor and spin with simply the spin-counting of the meson's spin degrees of freedom, except for neutral mesons where the additional content of the meson's flavor state function must also be coupled to by the quark-antiquark combination allowed by local flavor conservation.

iii) The 'knitting factors' N_i express the difficulty or probability of a quark and its 'neighbor' anti-quark coupling into the spatial wave function of a particular hadron. [It is conceptually somewhat akin to a hadronic decay factor in reverse]. We presume that all such knitting factors, whether the meson be a pion, kaon, η, η', ρ, ω, K^*, ϕ, etc., are all approximately the same. The units for N_i, as can be seen from the *Event*

Weight Function expression, are $(Energy)^{-2}$. The unitarity normalization constraint from the probability for the outermost hadron, as we shall see in Section 3, establishes all $N_i \simeq (75MeV)^{-2} \simeq (2.7fm)^2$.

iv) The transverse situation is described in terms of P_T of the observed hadrons, compatible with the description and handling of $A_{\text{world}-\text{surface}}$ above. (See Section 3 for our particular approach to possible local P_T compensation.)

In our modeling, the suppression of heavier particles arises from the mass of the hadron (as will be seen in Section 3), rather than from suppression factors at the quark pair production level and smaller knitting factors for vector mesons as, for example, Lund presumes.

The Lund modeling, by contrast, assumes:

i) At the virtual $q\bar{q}$ production stage, there is vertex suppression of $s\bar{s}$ production (the famous $s/u \simeq 0.3$), based on a WKB tunneling sort of argument; that is,

$$\nu_{u\bar{u}} \simeq \nu_{d\bar{d}} \simeq 1.0 \quad \text{and} \quad \nu_{s\bar{s}} \simeq 0.3$$

Also, for baryon production, the qq/q factor of ≈ 0.09 is introduced as a vertex suppression.

ii) As in our UCLA treatment, Clebsch-Gordon factors are different from 1.0 only, for example, to decide whether a $u\bar{u}$ state is to be coupled into a π^0, η, or η'.

iii) The knitting factors are used, via some detailed wave function arguments, for the Vector/All suppressions, with different parameters for light quarks, strange quarks, and heavy quarks. The final state phase-space spin-counting is also incorporated at this stage.

iv) The Lund modeling conceptually originates the P_T structure from balanced non-zero transverse momenta of a virtual quark-antiquark pair as it is created from the colorfield; however, this can be incorporated into the general description of eq(5).

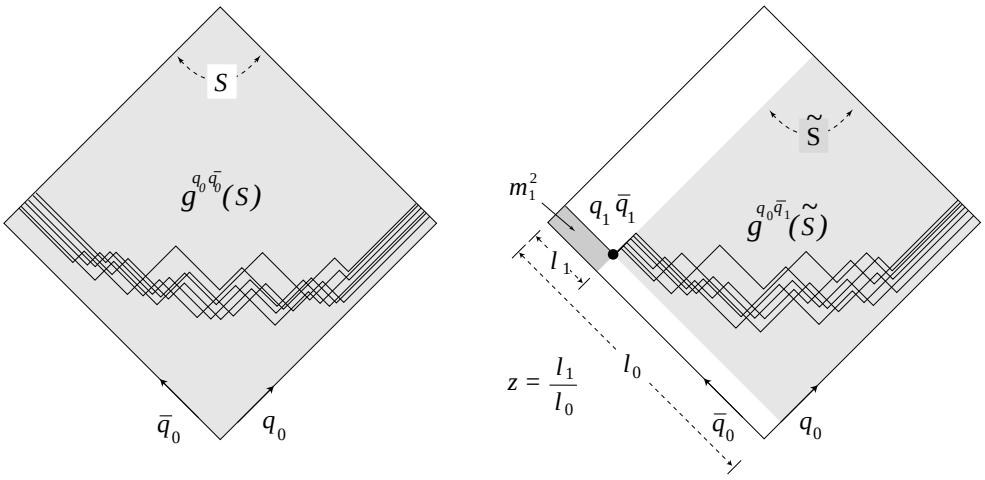

Figure 3: The probabilty that the first hadron is produced with a specific energy-momentum and flavor can be extracted by comparing $g^{q_0\bar{q}_1}(\tilde{S})$ (an *integration/summation* of the weight function for the rest of the system) to $g^{q_0\bar{q}_0}(S)$ (an *integration/summation* of the weight function for the original system). The primary $q_0\bar{q}_0$ with kinetic energy E will stretch until all kinetic energy is converted to potential energy, i.e., $2E = \kappa d$ where κ is the string tension (presumed constant) and d is the maximum separation between the primary $q_0\bar{q}_0$. This enables one to write distance and area in terms of energy and energy-squared respectively. For example, the energy-momentum fraction of the hadron z can be written in terms of the lengths l_1 and l_0 and the mass-squared of the first hadron can be recognized as the area labeled m_1^2 in the figure.

3 Deriving the Fragmentation Function dP_1 for the Outermost Meson from dW_f

- Define the *Total Weight* for all possible final state configurations at some value $S = E_{CM}^2$ by

$$\mathrm{g}^{q_0\bar{q}_0}(S) = \sum\!\!\!\!\!\!\int_f dW_f{}^{q_0\bar{q}_0}(S) \tag{6}$$

  where $\sum\!\!\!\!\!\!\int$ sums over all possible final state flavors and multiplicities and integrates over all possible momenta.

- Then:

$$dP_f{}^{q_0\bar{q}_0}(S) \equiv \frac{dW_f{}^{q_0\bar{q}_0}(S)}{\mathrm{g}^{q_0\bar{q}_0}(S)} \tag{7}$$

  is a properly normalized probability for an event of specified final state f such that

$$\sum\!\!\!\!\!\!\int_f dP_f{}^{q_0\bar{q}_0}(S) = 1$$

- Integrate eq(5) over the azimuthal angle of each hadron, introduce light cone variables W_+, W_-, and define

$$z_i \equiv \frac{(E_i + P_{z_i})_h}{(E + P_z)_{q_0}} \equiv \frac{W_{+_i}}{W_+} = \frac{l_1}{l_0} \tag{8}$$

  That is, z_i is the fraction of the initial quark's energy plus longitudinal momentum which the hadron carries. As is explained in the caption of Fig.3, the last step in eq(8) is due to the proportionality between the length and energy via a presumed approximately constant *string tension*.

- Note:

$$\delta\left(\mathbf{E} - \sum_i E_i\right)\ \delta\left(\mathbf{P}_z - \sum_i P_{zi}\right) = 2\delta\left(1 - \sum_i z_i\right)\ \delta\left(S - \frac{\sum_i (m_i^2 + P_{Ti}^2)}{z_i}\right)$$

  where the **bold face** signifies **total** quantity as before.

- This yields

$$dW_f{}^{q_0\bar{q}_0}(S) = \frac{N_1 C_1^2}{(4\pi)^2}\frac{dz_1}{z_1}e^{-\chi P_{T_1}^2}dP_{T_1}^2 \;\; \nu_{12} \times \ldots$$
$$\times\nu_{n-1,n} \;\; \frac{N_n C_n^2}{(4\pi)^2}\frac{dz_n}{z_n}e^{-\chi P_{T_n}^2}dP_{T_n}^2 \cdot (2\pi)^4\delta\left(1-\sum_{i=1}^{n} z_i\right)$$
$$\times\delta\left(S-\sum_{i=1}^{n}\frac{m_{T_i}^2}{z_i}\right)\delta\left(\mathbf{P}_x-\sum_{i=1}^{n}P_{x_i}\right)\delta\left(\mathbf{P}_y-\sum_{i=1}^{n}P_{y_i}\right) \;\; e^{-b'\mathcal{A}_{plane}} \quad (9)$$

- Next, one derives the outermost fragmentation function $dP_1^{q_0}(S)$ by writing out $dP_f^{q_0\bar{q}_0}(S)$ and then *integrating/summing* over all possible flavors, multiplicities, and momenta of all particles except the first (outer-most) one. But this *integration/summation* is simply $\mathrm{g}^{q_0\bar{q}_0}(\widetilde{S})$ where $\widetilde{S} = \left(S - m_{T_1}^2/z_1\right)(1-z_1)$ is the E_{CM}^2 of the system excluding the first hadron. The situation is indicated in Fig.3(a) and (b).

- Thus

$$dP_1{}^{q_0}(z_1, P_{T_1}^2, m_1^2) = \frac{N_1 C_1^2}{(4\pi)^2}\;\nu_{12}\; e^{-bm_1^2/z_1}\frac{dz_1}{z_1}\; e^{-\chi P_{T_1}^2}dP_{T_1}^2 \;\; \frac{\mathrm{g}^{q_1\bar{q}_0}(\widetilde{S})}{\mathrm{g}^{q_0\bar{q}_0}(S)} \quad (10)$$

  where $b = b'/\kappa^2$, $\kappa \simeq 1GeV/fm$ is the string tension, and m_1^2/z_1 is the part of the original area $\mathcal{A}(S)$ which is excluded from the new remaining area $\mathcal{A}(\widetilde{S}) = \widetilde{\mathcal{A}}$.

- The reason to introduce the *Event Weight Function* $dW_f^{q_0\bar{q}_0}(S)$, instead of using the probability $dP_f^{q_0\bar{q}_0}(S)$, is that a very useful theorem can be proven for $\mathrm{g}^{ij}(S)$[7]:

  > Take the natural log of both sides of eq(10). Differentiate with respect to S. Make the crucial assumption that the fragmentation function $dP_1^{q_0}(S)$ is, in fact, independent of S when S is large enough. Then, one obtains at large S
  >
  > $$\frac{S}{\mathrm{g}^{q_0\bar{q}_0}(S)}\;\frac{d\mathrm{g}^{q_0\bar{q}_0}(S)}{dS} = \frac{\widetilde{S}}{\mathrm{g}^{q_0\bar{q}_1}\left(\widetilde{S}\right)}\;\frac{d\mathrm{g}^{q_0\bar{q}_1}\left(\widetilde{S}\right)}{d\widetilde{S}}$$
  >
  > Separation of variables implies
  >
  > $$\mathrm{g}^{q_0\bar{q}_0}(S) = d_{q_0\bar{q}_0}S^a \quad \text{and} \quad \mathrm{g}^{q_1\bar{q}_0}(S) = d_{q_1\bar{q}_0}S^a \qquad (11)$$

where all systems have the same power 'a' of S^a and the coefficients d_{ij} depend on the flavors of the system.

- Thus, finally our fragmentation function for the outermost hadron is (as derived from dW_f with the one assumption that $dP_1^{q_0}(S)$ is independent of S at large S):

$$dP_1{}^{q_0}(z_1, P_{T_1}^2, m_1^2) = \frac{N_1 C_1^2}{(4\pi)^2}\,\nu_{12}\,(1-z_1)^a \left(1-\frac{m_1^2}{S z_1}\right)^a e^{-b m_1^2/z_1}\frac{dz_1}{z_1} e^{-\chi P_{T_1}^2} dP_{T_1}^2 \times \frac{d_{q_1\bar{q}_0}}{d_{q_0\bar{q}_0}} \tag{12}$$

where we have used $\widetilde{S} = \left(S - m_{T_1}^2/z_1\right)(1-z_1)$.

Note that an absolute normalization $N_1 C_1^2 \nu_{12}/(4\pi)^2$ is indicated for the fragmentation function in this derivation.

Though eq(12), with all $\nu_{ij} \simeq 1.0$ and all N_i approximately the same, is the primary structure to be used in the outside-in iterative implementation of our UCLA modeling, there are several important subtleties to be mentioned in its implementation:

a) Eq(12) contains an exponential suppression of P_T, carried over from the *Event Weight Function* of eq(5). At this stage in our work, we want simply to use some approximate P_T treatment which works so that we can focus on the question of meson production rates. We note that if one simply replaced m_H^2 by the transverse mass squared $m_T^2 = m_H^2 + P_T^2$, this would set $\chi = b/z$. However, one can show[8] that, if there are local compensation correlations between hadrons, then the subsequent P_T distributions will be narrower than the 'natural' distribution. In particular, in an outside-in implementation, if the P_T of one hadron is compensated for by the next n hadrons, then one can show that a factor of $n/(n-1)$ is introduced as a coeeficient of P_T^2 in the exponential. We find that the following works reasonably well and use it as an approximate treatment for the time being: (a) We use $n = 2$ (the most local compensation possible on the hadron level) so that the suppression factor is $\exp(-2bP_T^2/z)$; (b) After one hadrons P_T is picked, the next hadron's P_T is centered at -1/2 of the remaining P_T imbalance. This, as will be seen, gives an adequate description of the data. We also note,

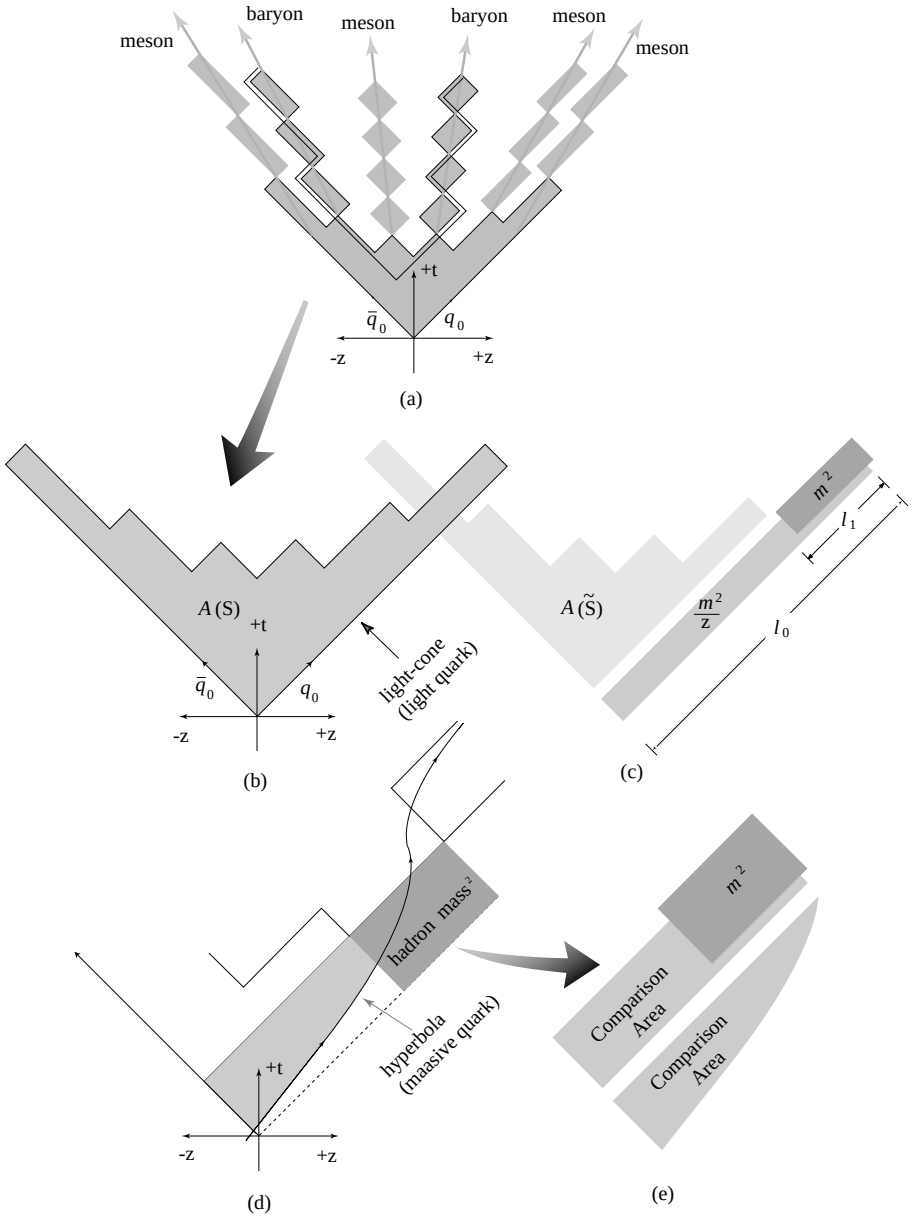

Figure 4: Various geometrical definitions to be used in deriving the outermost hadron's fragmentation function dP_1 are displayed. A heavy initial quark travels along a hyperbola rather than a light-cone, which affects the area involved. One has to modify the definition of z in order to incorporate this change.

however, that a different factor in $exp(-2bP_T^2/z)$ from $exp(-bm_H^2/z)$ leads to a small deviation from $Left - Right$ symmetry[2].

b) In Fig.2, we have presumed that the initial $q_0\bar{q}_0$ pair are quite light and essentially travel along the light cone. This is a good approximations for up, down, and even strange quarks. However, it is a poor approximation for charm and bottom quarks, which travel in a hyperbolic path inside the light cone. This is indicated in Fig.4. Focusing on area-law considerations, we presume that z_{eff} is really m_H^2/(comparison area) of Fig.4. This modifies the definition of the energy-momentum fraction z to be used in the exponential of eq(12), which arises from the area-law. The result is

$$z_{\text{eff}} = \frac{z}{1 - \frac{\mu^2 z}{m^2} - \frac{\mu^2 z}{m^2}\log\left(\frac{m^2}{\mu^2 z}\right)} \tag{13}$$

where μ is the current quark mass and m is the hadron mass. This has little effect on light and strange hadrons, but softens the predicted spectra for b-and c-hadrons in a manner which gives substantially better agreement with experimental spectra than otherwise.

c) The ratio $d_{q_1\bar{q}_0}/d_{q_0\bar{q}_0}$ correctly expresses a procedure which was clearly called for in our original phenomenological approach. Consider Fig.2: Let $\bar{q}_0$ be a $\bar{u}$, where we want to focus on properly picking meson #1 using our fragmentation function weights of eq(12). If $vertex_{12}$ is either $u\bar{u}$ or $d\bar{d}$, then meson #1 is non-strange. However, if $vertex_{12}$ is $s\bar{s}$, then *both* meson #1 and meson #2 are strange and therefore heavier than otherwise and therefore provide more suppression to the event via the $exp(-bm^2/z)$ factors. In our iterative phenomenological implementation, as we consider meson #1, we must *'look ahead'* at meson #2 also and incorporate the effects of the quark-antiquark flavor at vertex12 on the mass of meson #2; that is, we include a factor of

$$\sum\!\!\!\!\!\!\int_{\substack{i \\ z,P_T}} \frac{N_i C_i^2}{(4\pi)^2}\,\frac{(1-z)^a}{z}\left(1 - \frac{m_i^2}{Sz}\right)^a e^{-b\left(m_i^2 + 2P_T^2\right)/z}\, dz dP_T^2$$

from each appropriate meson #2 into the weight for each possible meson #1. The d_{ij} factors in eq(12) explicitly summarize and require this procedure.

More precisely, eq(12) can be recast into an eigenvector problem for the d_{ij}'s with the knitting factor N related to the eigenvalue: Since some first hadron must be created, there is a probability unitarity constraint of:

$$\sum\!\!\!\!\!\!\int_{\substack{z,P_T,\\ flavor}} dP_1{}^{q_0}(z, P_T^2, m^2) = 1$$

where the summation over $flavor$ is for the flavor of the hadrons containing a quark q_0. Carrying out this *sum/integration* over possible hadron flavors, z's, and P_T's and generalizing to any combination of initial quark and antiquark flavors leads to a set of coupled equations:

$$d_{ij} = \sum\!\!\!\!\!\!\int_{\substack{z,P_T\\ flavor}} \frac{NC_{ik}^2}{(4\pi)^2} \frac{(1-z)^a}{z} \left(1 - \frac{m_{ik}^2}{Sz}\right)^a e^{-b\left(m_{ik}^2 + 2P_T^2\right)/z} \, dz dP_T^2 \cdot d_{kj}$$

The factor quoted above which we use in the weight for hadron #1 from appropriate hadrons #2 is just the first step in an iterative solution to this eigenvector problem for the d_{ij}'s. Solving the eigenvector problem directly for our best fit values of $a = 1.65$ and $b = 1.18\ GeV^{-2}$, we find

$$d_{u\bar{u}} \simeq d_{d\bar{d}} \simeq d_{u\bar{d}} = d_{d\bar{u}}$$

$$d_{s\bar{u}} = d_{u\bar{d}} \simeq d_{s\bar{d}} = d_{d\bar{s}} \simeq 0.47\ d_{u\bar{u}}$$

$$d_{s\bar{s}} \simeq 0.47\ d_{s\bar{u}}$$

These, of course, to first order are simply the factors we have used for the hadron #2 weighting.

The solution to the eigenvalue problem also gives an intriguing new piece of information, namely, an eigenvalue for the knitting factor:

$$N \simeq 160 \sim 220 GeV^{-2} \simeq (68 \sim 80 MeV)^{-2} \simeq (2.5 \sim 2.9 \text{ fm})^2$$

The knitting factor appears to be a new and interesting concept, which may in some manner be related to the inverse of an hadronic decay constant. We note, in fact, that $N \simeq (2/f_\pi)^2$ for typical hadronic decay constants f_π of $110 \sim 160\ MeV$.

4 Baryon Formation

During our hadronization studies, as we have come to understand meson formation as apparently a very simple process, we have also come to view baryon formation as a much more complicated process: (1) three quarks must somehow coalesce into a baryon wave function; (2) whereas a quark and antiquark define a one-dimensional line between them in forming a meson, three quarks can have a more complex two-dimensional structure in forming a baryon; (3) one or more 'popcorn' mesons can be formed between the baryon and antibaryon; and (4) because of the multiple popcorn meson formation possible, there are many more combinations possible in the flavor chain of an event.

Recognizing this much-increased complexity for baryon formation, we extend our approach for mesons to baryon formation in as simple a manner as possible. The following approach works encouragingly well, though we currently must introduce at least one *'ad hoc'* parameter in order to reach fairly reasonable agreement with baryon rate, distribution, and correlation data:

1) For any given final state of hadrons with specified flavors and three-momenta, now including baryons and antibaryons, we assign a weight via the Event Weight Function approach. For this weight function, we presume:

2) The area law approach (and likewise proper kinematics) is valid.

3) The same values of *'a'* and *'b'* are used in the fragmentation function for baryons as for mesons.

4) There is no significant suppression for creating any number of virtual $u\bar{u}$, $d\bar{d}$, and $s\bar{s}$ pairs from the colorfield, as we also assumed for mesons.

5) To knit quarks into baryons:

   - Proper Clebsch-Gordon coefficients should be used for creating baryons as well as for mesons.
   - The spatial knitting factors to form baryons are assumed to be the same as for the mesons, where the *universal* value is found to be $\approx 1/(75MeV^2)$ from data and probability conservation, as is discussed in Section 3.

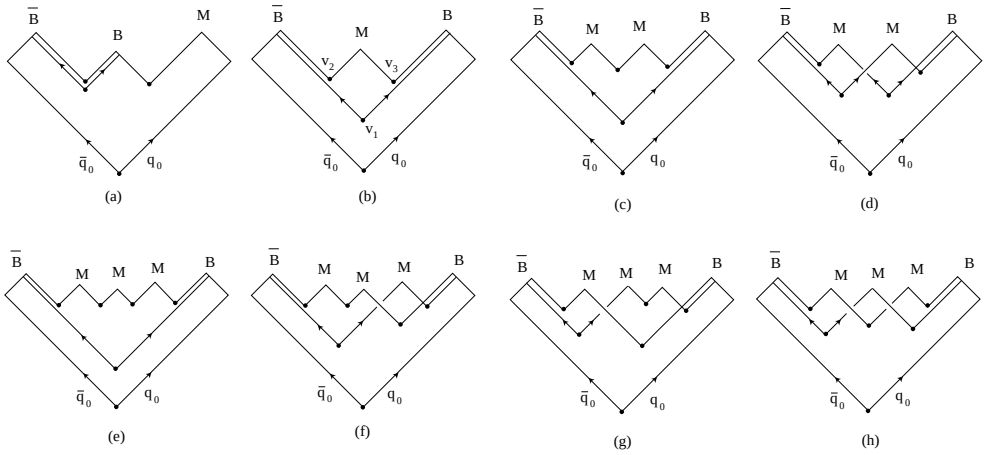

Figure 5: (a) The baryon and anti-baryon pair are produced adjacent to each other. (b) One popcorn meson is produced between the baryon and anti-baryon. (c)(d) Two possible ways of producing two mesons between the baryon and anti-baryon. (e)-(h) Four possible ways of producing three mesons between the baryon and anti-baryon. As more popcorn mesons are produced, the number of possible diagrams increases rapidly.

The Clebsch-Gordon coefficients for flavor and spin couplings are as simple for baryons as they are for mesons, presuming the three assumptions made in Section 2: (1) local flavor conservation in creating virtual $q\bar{q}$ pairs from the colorfield; (2) virtual $q\bar{q}$ pairs are available 'for free' from the colorfield; and (3) the spins of the final state hadrons are (at least, approximately) independent. Given these assumptions, the flavor coupling of whatever quarks are needed into the final state baryon flavor state is simply 1.0 and the spin coupling is simply the final state baryon spin degrees of freedom, i.e., 2.0 for spin 1/2 baryons and 4.0 for spin 3/2 baryons. The only difference between mesons and baryons is in the neutral sector: Mesons such as π^0, η, ρ^0, ϕ, etc. contain superpositions of different $q\bar{q}$ flavor states (i.e., $u\bar{u}$, $d\bar{d}$, and $s\bar{s}$) and therefore a given state of flavored $q\bar{q}$ (e.g., $u\bar{u}$) couples into a neutral meson flavor state with less than 1.0. By contrast, for example, every term in the Λ and Σ^0 flavor state is uds. Thus, the flavor coupling of quarks within the colorfield into *each* of the Λ and Σ^0 is 1.0.

In terms of area law treatment, because baryons contain three quarks, there is a new spatial degree of freedom. Whereas quark and antiquark in a meson always define a 1-dimensional line between them, the three quarks in a baryon can form a 2-dimensional spatial structure. As the three quarks propagate forward in time, an area law structure can take either a 'Y' structure or a 'Δ' structure connecting them[9]. In our current treatment, we presume that the area law for baryons can be treated in an approximate manner where the 'Y' or 'Δ' structure has been collapsed into a 1+1 dimensional structure (partially reminiscent of a diquark approach), as for mesons.

Even within the context of our presumed 1+1 dimensional treatment for baryons, another new degree of freedom emerges: namely, events where 'popcorn' mesons are 'popped out' between the baryon and antibaryon. Fig.5 shows (a) the baryon and antibaryon are adjacent and share two virtual $q\bar{q}$ pairs; (b) there is one intermediate popcorn meson and the baryon and antibaryon share one virtual $q\bar{q}$ pair; (c) there are two popcorn mesons and the baryon and antibaryon share one virtual pair (where the 'first' virtual pair must 'live a long time' before the rest of the baryon-antibaryon formation occurs); (d) there are two popcorn mesons in a 'crossed' diagram where the baryon and antibaryon share no virtual $q\bar{q}$ pairs; and (e)-(h) various diagrams with three popcorn mesons. Hypothetically, the popcorn diagrams, with ever increasing complexity, could extent to very many popcorn mesons. Note that the popcorn diagrams introduce new baryonic degrees of freedom which are otherwise unachievable, e.g., a $\bar{p} - \Xi$ (baryon-antibaryon) pair, and thus increase the density of final states for baryon production.

We find, in fact, that the series diverges as one increases the number of popcorn mesons. Thus we must introduce a parameter to effectively cut off long popcorn chains. We are led by the fact that strong interaction theory suggests a perimeter law as well as an area law (see Section 7). In the case of popcorn diagrams, where in fact the perimeters are longer than for non-popcorn diagrams, this suggests the use of a suppression of the form $exp(-\eta \cdot m_{popcorn})$. This works well phenomenologically with $\eta \simeq 3.5/GeV$.

5 Comparisons of Predictions with Data

Within the context of using JETSET7.4 (an outside-in iterative Monte Carlo program) to implement our approach, the comparisons of our model predic-

SECTOR	PARAMETERS	VALUE
Parton Shower	Λ (QCD strength)	0.32 GeV
	Q_0 (Cuts off shower)	2.0 GeV
P_T	n (Local correlations)	2
Heavy-quark Hadrons	(None needed)	
Light-quark Baryons	η (Controls popcorn)	3.5 GeV^{-1}
Light-quark Mesons	a (Growth of g(s))	1.65
	b (related to the *string tension*)†	1.18 GeV^{-2}

Table 1: Parameters for UCLA and their tuned values. Note that this set of parameters are tuned to span 10 GeV, 29 GeV and 91 GeV.
$\dagger$ $b = b'/\kappa^2$ where κ and b' are the *real* and the *imaginary* part (which allows a system to decay into the final state hadrons) of the string tension, respectively.

tions with data and the associated tuning of parameters naturally divide into five 'sectors' which are fairly separable, though there is some 'parameter cross-talk' between the sectors: (A) the parton shower; (B) P_T effects; (C) heavy-quark hadrons (containing c-or b-quarks); (D) light-quark baryons; and (E) light-quark mesons. Our main thrust in this paper is to make sure that (A)-(D) are well-tuned so that they create negligible biases and we can study the main focus of our investigation, namely (E) the light-quark meson production rates and distributions.

Comparisons are made at e^+e^- center-of-mass energies sufficiently high for hadronization studies, where there are large data samples from more than one detector, namely 91 GeV, 29 GeV, and 10 GeV (continuum). Data used include flavored multiplicities and distributions for the light-quark meson and baryon sectors, as well as for various topological and single particle distributions for the parton shower, P_T, and heavy-quark sectors.

For multiplicities, all relevant data through Summer 1996 have been included. At 10 Gev and 29 Gev, we use the data review by E. C. Berg

and C. D. Buchanan[10]; at 91 Gev, we use the 1995 data review by A. De Angelis[11], updated by publications and papers up through the ICHEP Conference at Warsaw in July 1996[12]. For the flavored distributions and for the topological and single particle distributions, a comprehensive (but not exhaustive) sample of relevant distributions gleaned from the same sources is presented. We concentrate most of these distribution displays at E_{CM} of $91GeV$ where the data is most copious.

Our predictions have been tuned simultaneously for all three center-of-mass energies with only the one set of energy-independent parameters cited in Table 1, which lists each *sector*, the major parameters used in tuning that sector, and the best-tune values of those parameters.

Once (A)-(D) (above) are reasonably well tuned, we reach our major conclusion in sector (E): *there are no significant deviations between our predictions and data at all three center-of-mass energies for all the various flavored light-quark meson rates and distributions studied, using only the two parameters – 'a' and 'b' – natural to the light-quark meson sector.*

It is also worthy of note that: (D) our current predictions for light-quark baryons, developed following an extension of our approach used for mesons, are approximately accurate (though not as good as for light-quark mesons) using only one additional *ad hoc* parameter; (C) our predictions for spectra of heavy-quark hadrons, which are substantially influenced by the area-law approach in our use of $z_{\rm eff}$, are rather good and require no additional parameters; and (A,B) our predictions for the topological distributions (dependent on the JETSET parton shower treatment and using the two major parameters therein) and for the various P_T distributions (using one *ad hoc* parameter) are also rather reasonable.

It is worth noting in the comparisons that there are some deviations between our predictions and data. The important questions to bear in mind are: (1) 'Are the deviations in the other sectors significant enough to affect the light-quark meson comparisons?' and (2) 'Are the deviations in the light-quark meson sector big enough to affect our conclusions?' We feel that the answer to each of these questions is 'No'. We also note that there are other treatments in the JETSET7.4 program which are approximations and which can affect the comparisons slightly. These include: the parton shower, the treatment during iteration to move past a gluon-created string-kink, the treatment of the final two hadrons at the end of the iteration, and

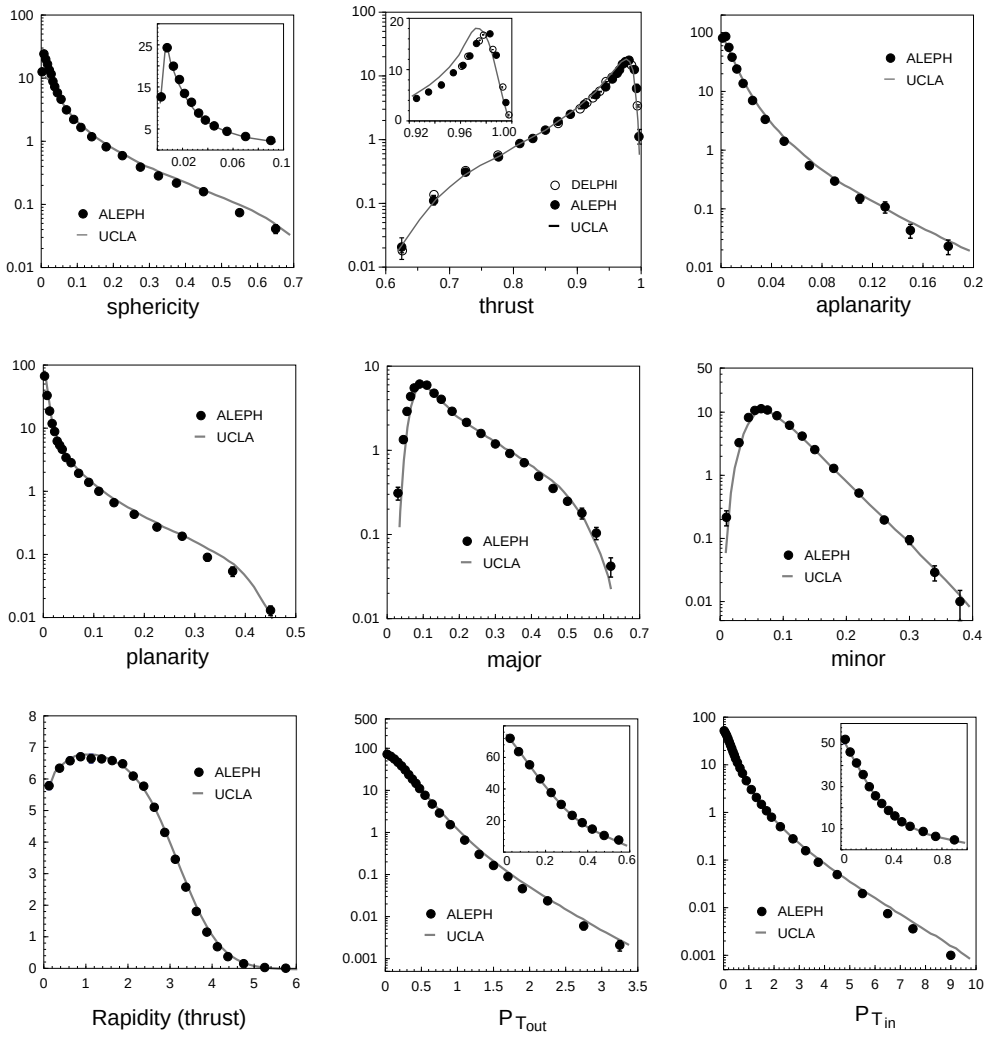

Figure 6: UCLA predictions for various topological variables and charged particle distributions are compared to LEP experiments at $E_{CM} = 91 GeV$.

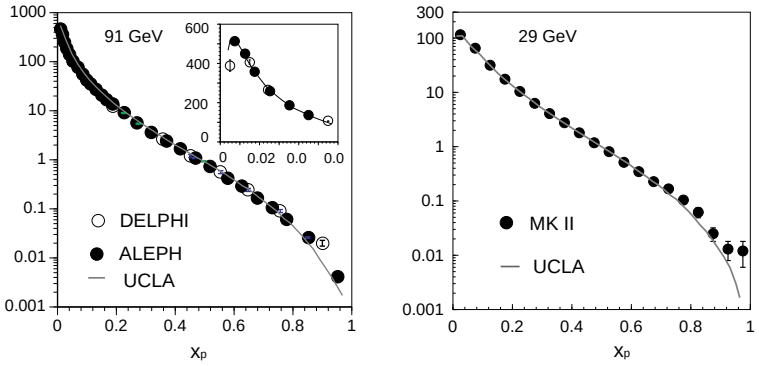

Figure 7: UCLA predictions for $X_P = P_{hadron}/P_{beam}$ of charged particles are compared to experiments at $E_{CM} = 29,\ 91\,GeV$.

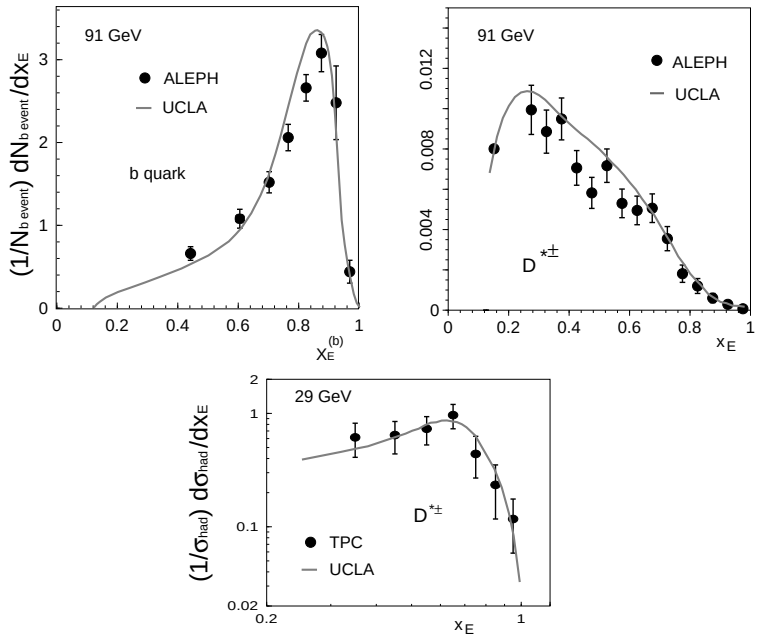

Figure 8: UCLA predictions for the heavy-quark hadrons are compared to experiments at $E_{CM} = 29,\ 91\,GeV$.

	91 GeV			29 GeV			10 GeV		
	DATA	UCLA	$STD^\dagger$	DATA	UCLA	$STD^\dagger$	DATA	UCLA	$STD^\dagger$
N_{ch}	20.92 ±0.24	20.62	0.94σ	12.57 ±0.26	12.79	-0.76σ	8.48 ±0.42	7.59	2.08σ
$\pi^\pm$	17.06 ±0.44	16.88	0.32σ	10.60 ±0.36	10.41	0.45σ	6.53 ±0.51	6.13	0.75σ
π^0	9.39 ±0.53	9.56	-0.31σ	5.84 ±0.28	5.96	-0.40σ	3.33 ±0.26	3.55	-0.82σ
$k^\pm$	2.37 ±0.13	2.24	0.88σ	1.444±0.080	1.490	-0.51σ	0.897±0.058	1.001	-1.63σ
k^0	2.012±0.033	2.038	-0.38σ	1.402±0.048	1.308	1.47σ	0.899±0.049	0.854	0.80σ
η	0.95 ±0.11	0.79	1.29σ	0.593±0.075	0.484	1.31σ	0.207±0.038	0.289	-2.05σ
η'	0.22 ±0.07	0.15	1.00σ	0.260±0.103	0.105	1.49σ	0.034±0.011	0.070	-3.22σ
ρ^0	1.29 ±0.13	1.16	0.93σ	0.846±0.054	0.723	1.93σ	0.353±0.064	0.425	-1.10σ
ω^0	1.11 ±0.14	1.02	0.61σ						
$k^{*\pm}$	0.713±0.056	0.791	-1.10σ	0.641±0.062	0.518	1.69σ	0.276±0.073	0.342	-0.88σ
k^{*0}	0.759±0.041	0.736	0.38σ	0.574±0.039	0.448	2.42σ	0.299±0.029	0.280	0.56σ
ϕ^0	0.107±0.009	0.126	-1.53σ	0.084±0.010	0.080	0.33σ	0.046±0.005	0.053	-1.13σ

Table 2: UCLA predictions for mesons at 10 GeV, 29 GeV and 91 GeV are compared to experiments.
† Decay table uncertainties are incorporated into the calculation of the number of standard deviations between the data and predictions, the column labeled *'STD'*. (See text.)

the tables used to decay higher-mass hadrons into those ultimately observed in a detector. Our very rough estimation is that these effects can lead to $2 \sim 10\%$ biases in the flavored multiplicities predicted.

5.1 Comparisons for parton shower, P_T, and heavy-quark hadrons

5.1.1 Parton shower

We use the parton shower option of JETSET7.4. This is a recipe which incorporates leading log parton shower structure with a weighting function to allow mimicking of the matrix element calculations for the first two perturbatively-calculated gluon emissions. It employs two somewhat correlated parameters Λ controlling the QCD running strength and Q_0 controlling the low-virtuality

cutoff at the end of the shower. Various 'topological' distributions, such as sphericity, thrust, aplanarity, planarity, major and minor eigenvalues of the sphericity tensor can be used to tune these parameters. A potpourri of such topological plots, as well as single charged particle distributions for rapidity and x_p, are displayed in Fig.6$\sim$7. The overall agreement seems quite acceptable , though there are minor discrepancies apparent at high thrust, high and low major values, and possibly high x_p.

5.1.2 P_T effects

If only transverse mass were involved in P_T effects, then we would use $\chi = b/z$ in eq(5) and eq(12). However, local P_T compensation between nearby hadrons, such as is discussed in Section 3 suggests a factor greater than 'one'. We use $\chi = 2b/z$, which approximates the most local P_T correlation possible. Agreement (see Fig.6) with data seem acceptably good, though our predictions might be a little high at high P_T values.

5.1.3 Spectra for heavy-quark hadrons

Our use of the area-law to derive $z_{\rm eff}$, as described in Section 3, leads to considerably softer spectra for heavy-quark hadrons than would otherwise be predicted. Using this, we find reasonable agreement with the observed spectra in both peak positions and in shapes (see Fig.8). This internally-consistent treatment would seem to eliminate the need to switch to the Peterson fragmentation function[13] for heavy-quark mesons.

5.2 Comparisons for light-quark mesons

[Note: We defer the discussion of light-quark baryons, which are influenced by *'a'* and *'b'* of the fragmentation function as well as by the ad hoc *popcorn* parameter η, until after the light-quark meson discussion. Roughly speaking, the light-quark meson data are used to tune *'a'* and *'b'* and then η is used to tune to the baryon data.]

This light-quark meson sector is our most important study of *'elementary fundamental'* behavior of the colorfield. This sector is predominantly controlled by only the two 'natural' parameters of the fragmentation function for the modeling – 'a' from the growth of g(S) with S and 'b' which is related

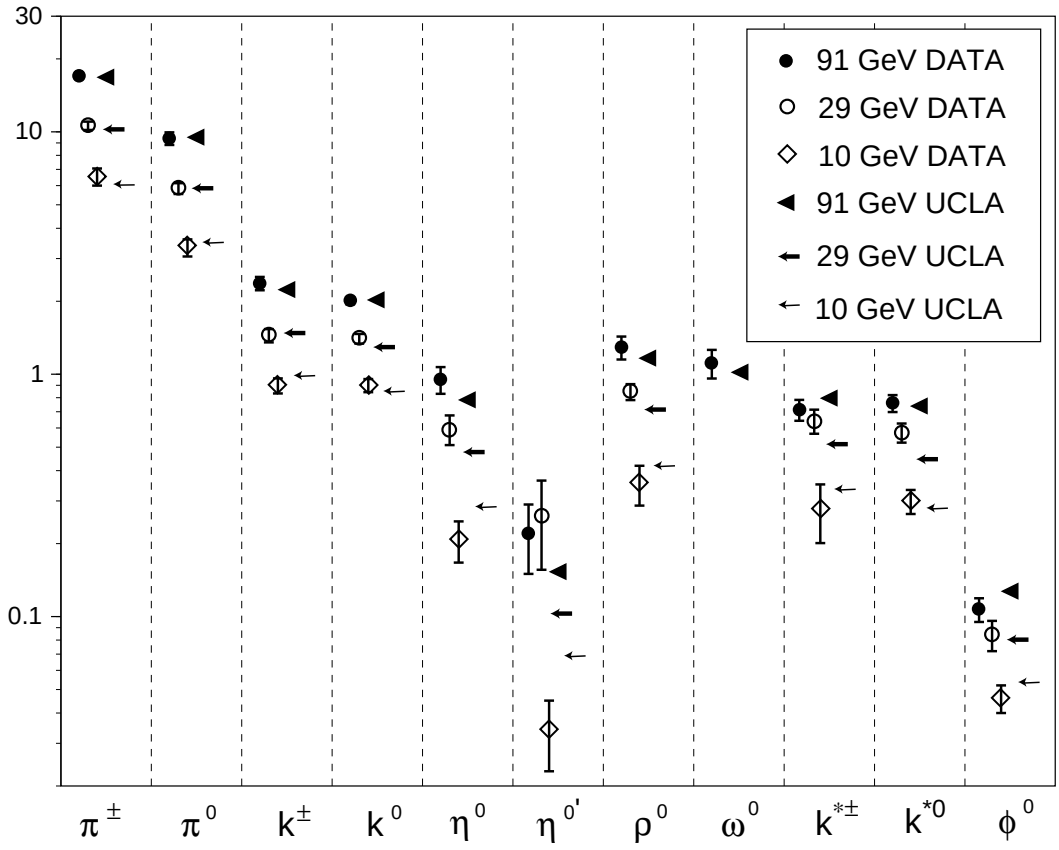

Figure 9: Comparison of the experimental and predicted absolute production rates per event for various flavored light-quark mesons at $E_{CM} = 10$, 29, and 91 Gev.

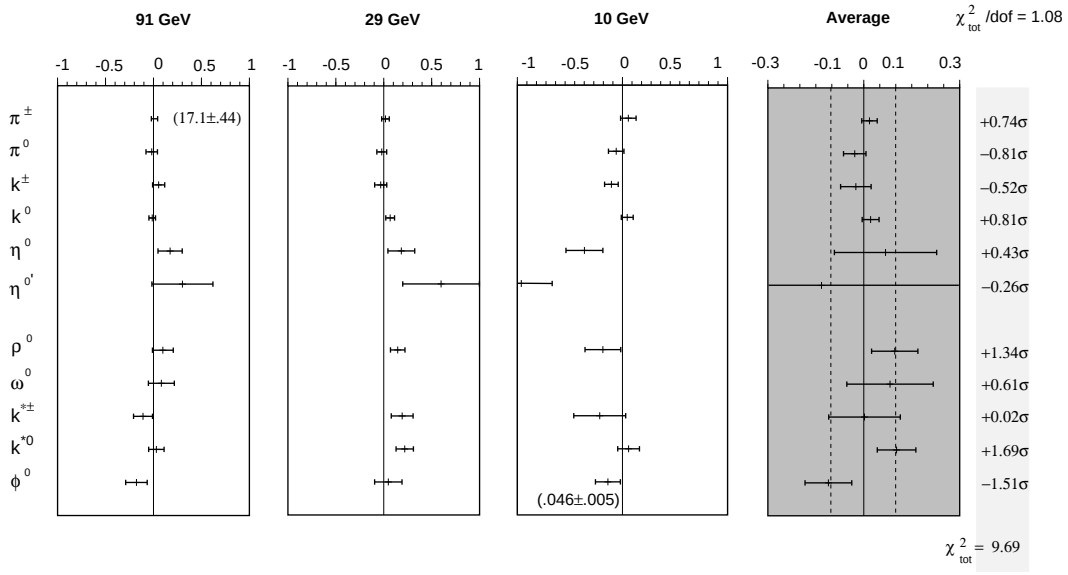

Figure 10: The summary of experimental data vs. UCLA prediction for mesons at $E_{CM} = 10,\ 29,\ and\ 91\,GeV$. On the right, in an *expanded* scale, the comparison is shown for each flavor meson averaged over all three energies.

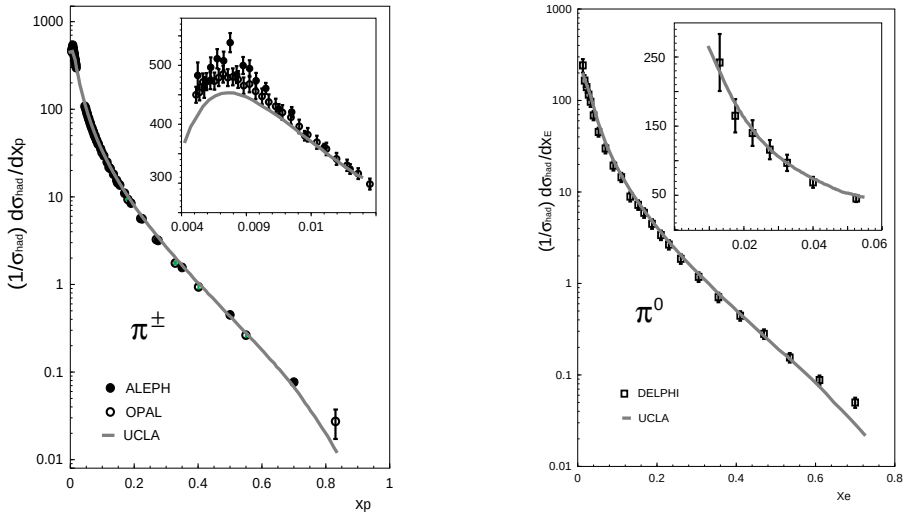

Figure 11: UCLA predictions for π mesons are compared to experiments at $E_{CM} = 91\,GeV$.

to the imaginary part of the string tension which allows the system to decay.

Our predicted multiplicities are compared with data for various pseudoscalar and vector mesons at E_{CM}=91, 29, and 10 GeV in Table 2 and in Fig.9 and 10.

Fig.9 compares the absolute magnitudes of predicted and measured multiplicities and gives an overall view of the range of rates over which prediction and experiment are compared. Fig.10 provides a finer grain comparison by suppressing the absolute rates and displaying deviations simultaneously in both percent and standard deviations. We use 'data minus prediction' to determine the $\pm$ sign in our presentations of standard deviations.

Though the uncertainties quoted for the data in Table 2 are simply the experimental uncertainties, in the comparisons with predictions in Table 2 (the column labeled *'STD'*) and in Figs.9 and 10, we have included in quadrature estimations of the effects on the multiplicity-comparison uncertainties arising from the decay table uncertainties. [That is, if the decay table rate of a particle decaying into a relevant particle is incorrect, then the predicted rate

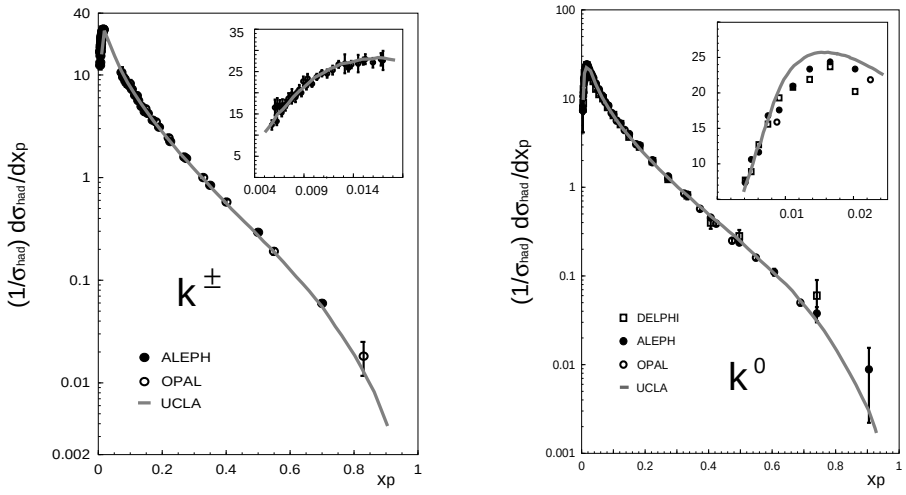

Figure 12: UCLA predictions for k mesons are compared to experiments at $E_{CM} = 91\,GeV$.

for that relevant daughter particle will be biased. If the decay table rate is incorrect for a decay mode used experimentally to reconstruct the multiplicity for a relevant particle, then the experimental rate found will be biased. We have presumed the uncertainties in multiplicity comparisons from these decay table uncertainties to be: $\pm 2\%$ for pions; $\pm 3\%$ for kaons; $\pm 4\%$ for ρ^0 and ω^0; $\pm 6\%$ for η, η', k^0 and $k^{\pm}$; and $\pm 8\%$ for ϕ; also, $\pm 1\%$ for $N_{\rm charged}$.]

Comparing data and predictions over the range of meson multiplicities from 17.1 $\pi^{\pm}$ at 91 Gev to 0.046 ϕ's at 10 Gev (a range of ~ 400), we arrive at our Report's most important conclusion, namely: *Over this broad range, there are no deviations which seem truly significant.*

If we presume that our model is accurate (and the deviations appear to be fairly randomly distributed), then we can treat the comparisons of the same meson at different energies as different measurements of the same quantity. Using both fractional deviations and standard deviations, these can be combined appropriately to give an overall comparison for each meson. This is displayed in the right-hand column of Fig.10, which employes an *expanded* scale, since the deviations are small. As displayed, there is very little difference between data and prediction; each flavor is typically within

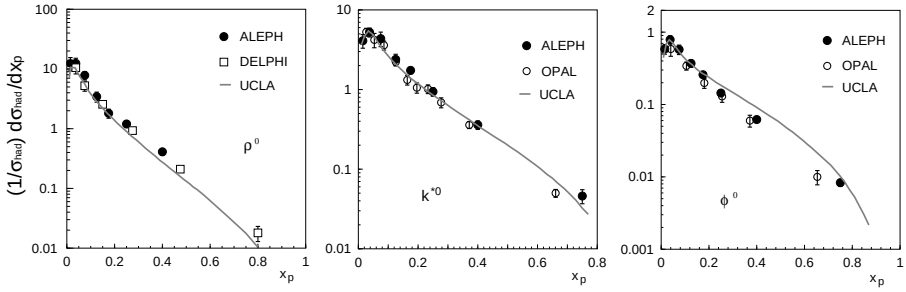

Figure 13: UCLA predictions for ρ^0, k^{*0}, and ϕ mesons are compared to the experiments at $E_{CM} = 91\,GeV$.

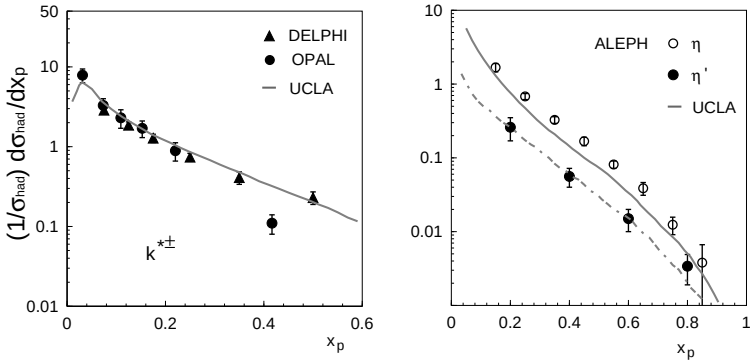

Figure 14: UCLA predictions for $k^{*\pm}$, η and η' mesons are compared to experiments at $E_{CM} = 91\,GeV$.

	91 GeV			29 GeV			10 GeV		
	DATA	UCLA	$STD^\dagger$	DATA	UCLA	$STD^\dagger$	DATA	UCLA	$STD^\dagger$
P	0.98 ±0.10	0.97	0.09σ	0.570 ±0.036	0.498	1.81σ	0.275 ±0.034	0.196	2.26σ
Λ^0	0.373 ±0.008	0.383	-0.70σ	0.209 ±0.010	0.197	1.02σ	0.080 ±0.014	0.079	0.07σ
$\Sigma^\pm$	0.182 ±0.019	0.119	3.01σ						
Σ^0	0.070 ±0.012	0.092	-1.79σ						
Ξ^-	0.0262±0.0010	0.0204	3.52σ	0.0176±0.0034	0.0106	2.99σ	0.0059 ±0.0009	0.0045	1.48σ
Δ^{++}	0.124 ±0.065	0.094	0.46σ	0.094 ±0.094	0.049	0.48σ	0.040 ±0.010	0.019	2.06σ
$\Sigma^{*\pm}$	0.047 ±0.005	0.074	-4.86σ	0.0330±0.0094	0.0359	-0.30σ	0.0107 ±0.0020	0.0133	-1.26σ
Ξ^{*0}	0.0058±0.0011	0.0073	-1.25σ	0.0052±0.0040	0.0035	0.42σ	0.0015 ±0.0005	0.0013	0.40σ
Ω^-	0.0013±0.0003	0.0006	2.19σ	0.0053±0.0032	0.0003	1.56σ	0.00072±0.00038	0.00010	1.62σ

Table 3: UCLA predictions for the baryons at 10 GeV, 29 GeV and 91 GeV are compared to experiments.
† The decay table uncertainties are incorporated into the calculation of the number of standard deviations between the data and predictions, the column labeled *'STD'*. (See text.)

$\pm 10\%$ and/or $\pm 1.0\ \sigma$. These energy-averaged flavor comparisons have an overall $\chi^2/d.o.f. = 9.69/9 = 1.08$ or an average of ~ 1.0 standard deviation.

Fig.11$\sim$14 display sample energy and momentum distributions for various flavors at $E_{CM} = 91 GeV$. Again, though there are minor differences, the overall agreement seems good.

Overall, we find that our predictions for light-quark meson rates and distributions are reasonably accurate and appear to display no significant deviations from the data over integrated multiplicity rates ranging from 17/event to .046/event (a range of ≈ 400) and over differential rates in $1/\sigma_{\rm TOT} \cdot d\sigma/dx_p$ ranging from 500 to 0.01 (a range of $\approx 50,000$).

5.3 Comparisons for light-quark baryons

Baryons are much more complicated objects than mesons and their physical dynamics are much less clear. E.g., three virtual quark-antiquark pairs must

be created from the colorfield and, via some dynamics, the three quarks must knit together into a baryon; *popcorn* mesons can be formed between the baryon and antibaryon, which radically increases the number of ways in which a given set of final state hadron flavors and momenta can be achieved.

For baryon production we follow an extrapolation of our successful meson production approach in order to see whether this sort of approach makes sense for baryon production: We use our Event Weight Function (a) incorporating the area-law, (b) presuming no suppression for creating any number of $u\bar{u}$, $d\bar{d}$, or $s\bar{s}$ virtual pairs from the colorfield, (c) assuming the spatial knitting factors for baryon formation are the same as for meson formation, and (d) developing the necessary Clebsch-Gordon coupling apparatus for the flavor and spin coupling. Since we follow a Fermi Golden Rule addition of final states type of approach, the possibility of long chains of *popcorn* mesons increases the rates of baryon production. Currently, we introduce a parameter η in $\exp(-\eta\, m_{pop})$, motivated by QCD-inspired perimeter law arguments (see Section 4), to cut off these long chains.

Our goals currently in studying baryons are: (1) to show that this sort of approach has potential merit, (2) to tune the baryon sector predictions to the data well enough that they won't create any biases in the meson studies, and (3) to point the way toward the kind of data needed to really understand baryon production.

We find that indeed this approach works rather well. Thus our baryon modeling, though clearly not yet as fundamental as for mesons, provides a very good platform for further developing our understanding of baryon formation on a fundamental level as significantly higher quality data becomes available.

Our baryon multiplicity comparisons are summarized in Table 3 and Figs.15 and 16, paralleling Table 2 and Figs.9 and 10 for light-quark mesons. The decay table uncertainties presumed are: $\pm 3\%$ for protons and lambdas; $\pm 5\%$ for $\Sigma^{\pm}$, Σ^{0}, Ξ^{-}, Δ^{++} and $\Sigma^{*\pm}$; and $\pm 8\%$ for Ξ^{*0} and Ω^{-}. Fig.17$\sim$18 display various single baryon distributions.

Fig.19 displays the baryon-antibaryon rapidity correlation for $\Lambda\bar{\Lambda}$ pairs[14]. Table 4 displays baryon-antibaryon, baryon-baryon, baryon-meson, and meson-meson correlation rates.

The single-particle rates vary from ≈ 1.0 for protons at 91 GeV to $\approx .001$

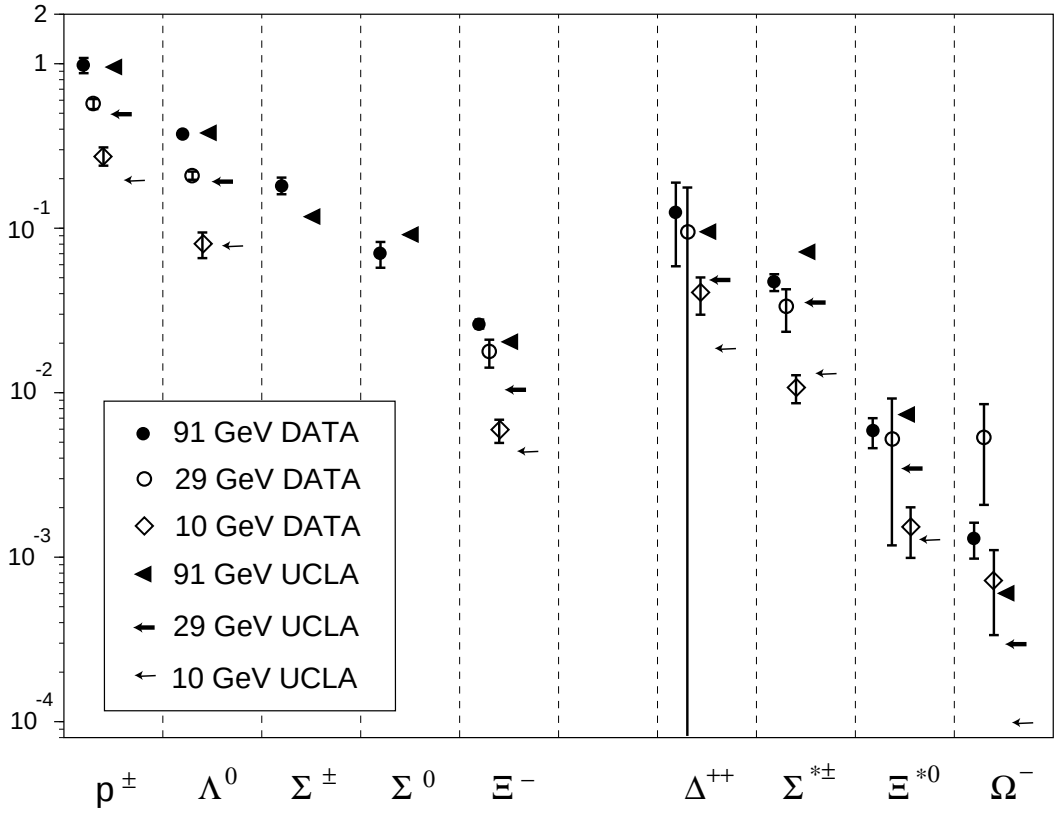

Figure 15: Comparison of the experimental and predicted absolute production rates for various flavored baryons at $E_{CM} = 10$, 29, and 91 Gev.

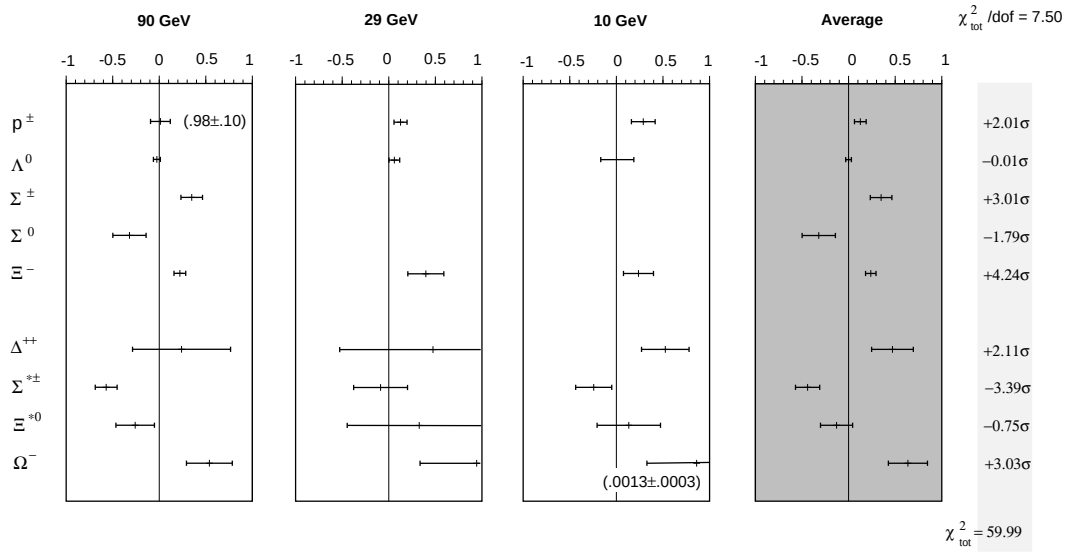

Figure 16: The summary of UCLA prediction vs. experiments for the baryons at $E_{CM} = 10,\ 29,\ and\ 91\,GeV$. On the right, the comparison is shown for each flavor baryon averaged over all three energies.

	DATA	UCLA
$\Lambda\bar{\Lambda}/evt$	$0.089 \quad \pm 0.007$	0.114
$\{\left(\Xi^-\bar{\Lambda} - \Xi^-\Lambda\right) + \left(\bar{\Xi}^+\Lambda - \bar{\Xi}^+\bar{\Lambda}\right)\}/evt$	$0.0096 \ \pm 0.0023$	0.0146
$\{\Xi^-\bar{\Xi}^+ - \left(\Xi^-\Xi^- + \bar{\Xi}^+\bar{\Xi}^+\right)\}/evt$	0.00038 ± 0.00067	0.00128
$\left(\Lambda\Lambda + \bar{\Lambda}\bar{\Lambda}\right)/evt$	$0.0249 \ \pm 0.0022$	0.0272
$\left(\Lambda k_s^0 + \bar{\Lambda}k_s^0\right)/evt$	$0.403 \quad \pm 0.029$	0.394
$k_s^0 k_s^0/evt$	$0.593 \quad \pm 0.036$	0.628

Table 4: Baryon-antibaryon, baryon-baryon, baryon-meson and meson-meson correlation rates at Ecm=91 Gev.

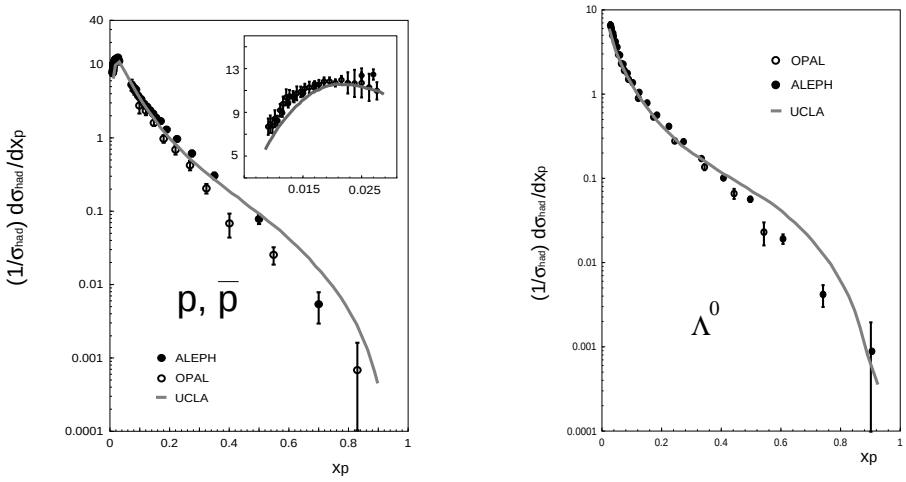

Figure 17: UCLA predictions for protons and Λ baryons are compared to experiments at $E_{CM} = 91\,GeV$.

for Ω^- at 10 GeV. Generally, the predictions follow the data fairly well. However, we seem systematically to *underpredict* the rates for Ξ^-'s and Ω^-'s and possibly protons and to *overpredict* the rates for $\Sigma^{*\pm}$.

Other intriguing deviations in baryon production include: (a) As displayed in Fig.17 and 18, we consistently *overpredict* the baryon production above $x_p \simeq 0.5$. (This phenomenon lead to the *'leading baryon suppression'* factor recently introduced into JETSET.) (b) Our predicted $\Lambda - \bar{\Lambda}$ rapidity correlation in Fig.19 is not sharp enough and is too broad (e.g., suggesting somewhat too much popcorn in our Monte Carlo). However, (c) our predictions of the absolute baryon-antibaryon correlation rates (see Table 4) are too high, suggesting too little popcorn (whereas we note that our predicted baryon-baryon, baryon-meson, and meson-meson correlation rates agree adequately with the data).

To bring the understanding of baryon formation to the same, apparently fundamental, level as our current meson formation understanding will require $\approx 10^8\ e^+e^-$ annihilation events with good, relatively unbiased, efficiency and particle identification in order to obtain flavor-identified three-body baryon-meson-antibaryon rapidity correlations. This appears to be achievable only

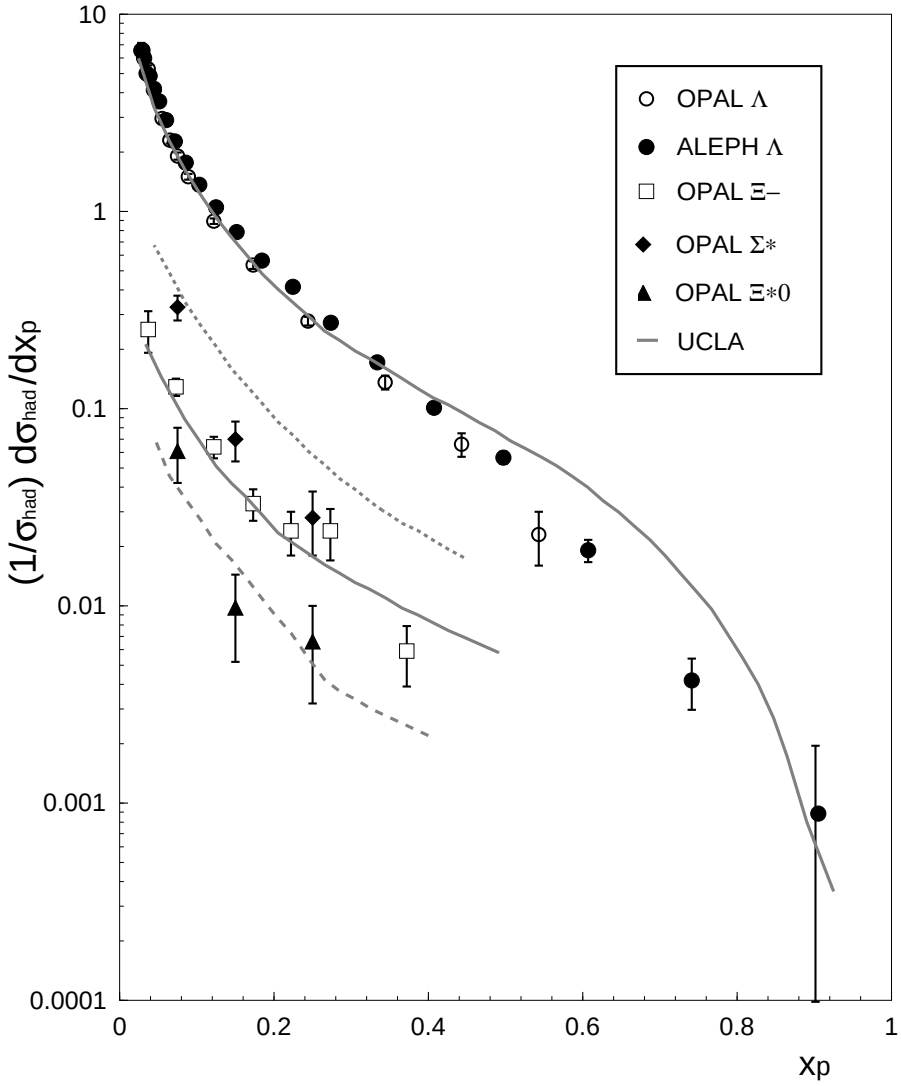

Figure 18: UCLA predictions for various strange baryons are compared to experiments at $E_{CM} = 91\,GeV$.

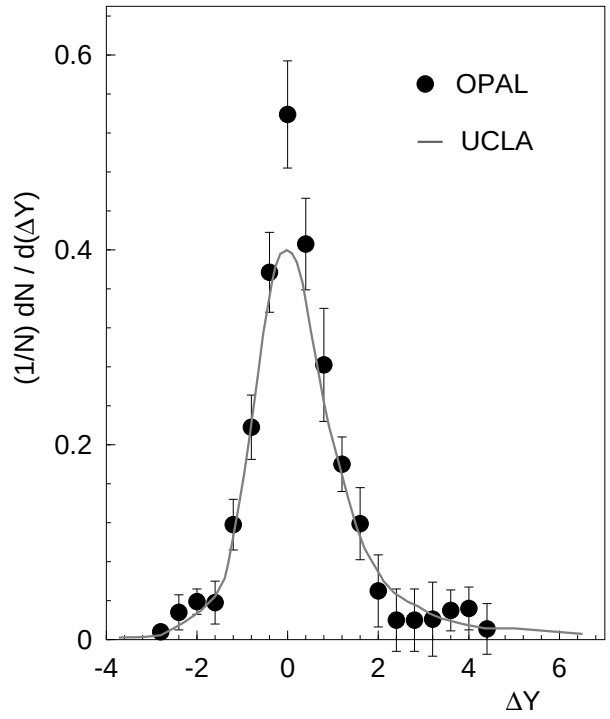

Figure 19: UCLA prediction for the rapidity correlation of Λ and $\bar{\Lambda}$ baryon pair is compared to experiments at $E_{CM} = 91\,GeV$.

with the continuum events from one of the high luminosity B factories currently being built.

6 Connections with QCD

When one has a successful phenomenology, there are two possible approaches toward deeper understanding: (1) Working *'backwards'* from the phenomenology with as few assumptions as possible to see what kind of a theory might justify the phenomenology, or (2) Hypothesizing a theory and then working *'forward'* to see if (or under what conditions) it leads to the phenomenology. Since QCD exists as a very strong candidate for the theory underlying hadronization, we will work primarily in the second mode to see to what extent QCD can justify our *Event Weight Function* for hadronization.

There are two main questions to try to answer from QCD:

- To justify the structure of the *Event Weight Function*: i.e., the space-time area law, the limited transverse phase-space, the possible vertex suppression factors, and the Clebsch-Gordon and spatial knitting factors.

- To estimate the sizes of the vertex suppression factors and knitting factors.

Ultimately, one would then hope to extend the treatment to include understanding of P_T, of baryon formation, etc.

Lattice QCD work[15] within a Euclidean space-time metric indicates that, as a quark and antiquark separate, the color-field begins to collapse into a narrow tube-like structure – approximately a *'string'*. There is some very preliminary lattice-work indication[16] that, if virtual quark-antiquark pair production is allowed from the colorfield, then the energy density near the center of the string begins to drop – that is, the string begins to break. This, of course, is also bolstered by the very strong intuition that as a string stretches, a string broken by a quark-antiquark pair represents a lower energy state and therefore that *the string prefers to break*.

Even if one can't expect truly quantitative results from this analytic tool due to the difficulties of extracting the behavior in the continuum limit and of extrapolating from a Euclidean metric to a Minkowskian one, the strong

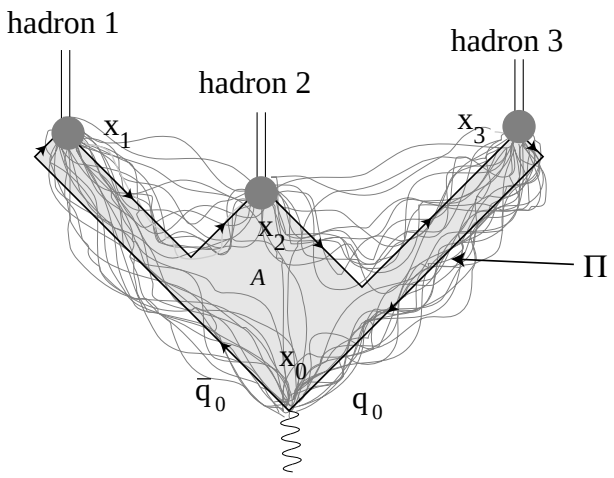

Figure 20: The virtual photon created by the e^+e^- annihilation decays into the initial $q_0\bar{q}_0$ at x_0. Three hadrons are produced at $x_1,\ x_2,\ x_3$ where the solid straight lines Π depict the classical trajectories of massless fermions (quark or anti-quark) whereas gray lines depict all possible loops connecting the four points $x_0,\ x_1,\ x_2,\ x_3$.

coupling expansion can provide some insights about the physics typical to the strong coupling domain which otherwise would not be possible. For this purpose, we sketch (below) the relevant results of lattice QCD without extensive derivation or justification in order to demonstrate what *lattice QCD* can suggest. (See [17], accepted for publication in Physics Reports for a more extensive discussion.)

To the lowest order in QED, the cross section $e^+e^- \to f$, where f is a final state of hadrons with particular momenta and flavors can be written as

$$\sigma_{e^+e^-\to f} = \frac{8\pi^2\alpha^2}{S^3}(2\pi)^2\delta\left(P_1 + P_2 - P_f\right) l_{\mu\nu}\langle f|J^\mu(0)|0\rangle\langle f|J^\nu(0)|0\rangle^* \qquad (14)$$

where $l_{\mu\nu}$ is the lepton current of an electron and J^μ is an electromagnetic current. The matrix element $\langle f|J^\mu(0)|0\rangle$ is related to an *n-point Green's function*. For example, as displayed in Fig.20, a 4-point function, with a loose notation, can be written as

$$\langle f|J^\mu(0)|0\rangle \sim \langle 0|T\bar{\psi}_0\psi_0\bar{\psi}_1\psi_1\bar{\psi}_2\psi_2\bar{\psi}_3\psi_3|0\rangle \sim G\left(x_0, x_1, x_2, x_3\right) \qquad (15)$$

where indices for the quark fields 1, 2, 3 indicate the production points of hadrons and 0 indicates the origin where the virtual photon couples to the current J^μ. The next step is to evaluate the n-point Green's function in Euclidean Lattice QCD.

In general, there are many different ways to construct QCD action on the lattice space-time; the *Wilson action* is[18]

$$\begin{aligned} S(U,\bar{\psi},\psi) &= \frac{6}{\mathrm{g}^2}\sum_{\Box}\left(1-\frac{1}{3}Tr\left(U_\Box + {U_\Box}^\dagger\right)\right) + a^3\sum_n \bar{\psi}_n(4+ma)\psi_n \\ &-\frac{a^3}{2}\sum_{n,\mu}\bar{\psi}_n\{(1+\gamma_\mu)\,U\,(n+\hat{\mu},-\mu)\,\psi_{n+\hat{\mu}} + (1-\gamma_\mu)\,U\,(n-\hat{\mu},\mu)\,\psi_{n-\hat{\mu}}\} \\ &= \sum_{i,j}\bar{\psi}_i K_{ij}(U)\psi_j + S_G \end{aligned} \tag{16}$$

where $U_\Box$ is the product of links connecting four nearest sites (a *'plaquette'*), μ denotes the space-time index, a is the lattice spacing, and g is the bare coupling constant. The matrix

$$K_{ij} \equiv (8+2ma)\delta_{ij} - (1+\widehat{e}_\mu\gamma_\mu)U_{ij} = \frac{1}{\kappa}(\delta_{ij} - \kappa M_{ij})$$

was introduced with the hopping parameter $\kappa = 1/(8+2ma)$ in eq(16).

Upon introducing source terms $(\rho,\bar{\rho})$ and integrating out the fermion fields, the n-point Green's function becomes

$$\begin{aligned} Z(\rho,\bar{\rho}) &= \int (dU)\; det\; K\; \exp\left(\sum_{ij}\bar{\rho}_i K^{-1}_{ij}\rho_j\right)\; e^{-S_G(U)} \\ &= \int (dU)\; \exp\left(\sum_{ij}\bar{\rho}_i K^{-1}_{ij}\rho_j\right)\; e^{-S_G(U)} \end{aligned} \tag{17}$$

where the *Quenched approximation* ($det\; K = 1$; that is, no closed internal quark loops) was used in the last step.

Then, the 4-point function eq(15) can be written using eq(17) as:

$$\begin{aligned} G\,(x_0,x_1,x_2,x_3) &= \frac{1}{Z}\int\left(dU d\bar{\psi} d\psi\right) T\left(\bar{\psi}_0\psi_0\bar{\psi}_1\psi_1\bar{\psi}_2\psi_2\bar{\psi}_3\psi_3\right)\; e^{-S\left(\psi,\bar{\psi},\rho,\bar{\rho},U\right)} \\ &= \frac{1}{Z(\rho,\bar{\rho})}\frac{\partial Z(\rho,\bar{\rho})}{\partial\rho_0\cdots\partial\rho_3\partial\bar{\rho}_0\cdots\partial\bar{\rho}_3}\bigg|_{\rho=0} \\ &= \int (dU)\left(K^{-1}_{01}\cdots K^{-1}_{30} + \text{permutations}\right)e^{-S_G} \end{aligned} \tag{18}$$

By an iteration, the inverse matrix K^{-1} identically becomes

$$K_{ij}^{-1} = \kappa \left(\delta_{ij} + K_{ik}^{-1} M_{kj} \right) = \kappa \left(\sum_{l=0}^{\infty} \kappa^l M^l \right)_{ij} \tag{19}$$

Thus, K^{-1} will include the product of $(1 \pm \gamma_\mu) U$. One, then, finds the important result that eq(18) becomes

$$\begin{aligned} G\left(x_0, x_1, x_2, x_3\right) &\propto \sum_C \kappa^m \int (dU)\ Tr\ (U \cdots U)_C\ e^{-S_G} \\ &= \sum_C \kappa^m\ \langle P\ e^{ig \oint_C dx^\mu A_\mu} \rangle_{gluon} \end{aligned} \tag{20}$$

where m is the perimeter p of the loop C in lattice units, A_μ is the gauge field, and P stands for *path ordered product*. The summation runs over all the loops connecting the four points. The quantity in brackets $\langle \cdots \rangle$ is the expectation value of the *Wilson Loop* over the *gluon field*.

Now, when the coupling gets weak (and therefore the lattice spacing gets small), the perimeter dependence still persists, in the form of $e^{-\mu\, p/a}$, since it represents the dependence of the fermion's internal energy, while the area dependence collapses and overall Wilson Loop average yields *Coulomb's law*. So, for weak coupling (the early perturbative region) the exponent diverges as $a \to 0$ and dominates the Green's function in this limit. The energy of the initial $q_0 \bar{q}_0$ pair is so large that their coupling to gluons can be considered to be small. Therefore, this perimeter dominance overwhelmly chooses the light-cone as its trajectory in order to minimize the perimeter. Thus, this eliminates all other terms in eq(20) except a term with a loop Π which goes through the light-cone as in Fig.20, i.e.,

$$\begin{aligned} G\left(x_0, x_1, x_2, x_3\right) &\propto \sum_C \kappa^m \int (dU)\ Tr\ (U \cdots U)_C\ e^{-S_G} \\ &\simeq \kappa^m\ \langle P\ e^{ig \oint_\Pi dx^\mu A_\mu} \rangle_{gluon} \end{aligned} \tag{21}$$

Next, once the initial $q_0 \bar{q}_0$ are separated far away from each other defining a *loop* Π, the coupling rapidly becomes strong, leading toward the hadronization process. The expectation value of the Wilson Loop over the gluon field in eq(21) should be evaluated considering that the coupling is a mixture of weak (near the edge of the primary $q_0 \bar{q}_0$) and strong (in the middle) over

the configuration Π in Fig.20. But the expectation value of the Wilson loop over the gluon field evaluated over the weak coupling region is essentially *common* to all events with different hadronic final states [see below for the comments about UCLA 'stage 3']; hence the expectation value over the gluon field in eq(21) can be evaluated as if the coupling is strong in all regions of configuration Π in Fig.20 using the *strong coupling expansion*. [Note that the expectation value of the Wilson loop evaluated over the weak coupling region can be considered as a *weak coupling correction* to the expectation value of the Wilson loop evaluated using strong coupling throughout the configuration Π. Further, since this *correction* factor is essentially *common* to all hadronic final states (in 1+1 dimensions, it is exact), it therefore cancels in comparing the *relative* weights of the *Event Weight Function* for different final states or when using the *fragmentation function* eq(12).]

This yields an area dependence

$$\left(\mathrm{g}^2\right)^{-\mathcal{A}/a^2}$$

Thus, finally, one finds the important result in Euclidean space-time with lattice spacing a:

$$G\left(x_0, x_1, x_2, x_3\right) = \kappa^{p/a} \left(\mathrm{g}^2\right)^{-\mathcal{A}/a^2} \tag{22}$$

where $\mathcal{A}$ is the minimal area enclosed by the loop Π, p is its perimeter, and a is the lattice spacing.

The above procedure is, in fact, a dual expansion in terms of $1/(4+ma)$ (a *hopping parameter*) which gives a multiplication of successive link variables (the perimeter dependence) and a coupling constant g which gives a rule for tiling the surface with *plaquettes* (the area dependence). So, one can see there is always a competition between area dependence and perimeter dependence.

The fact that the expectation value of the Wilson loop over the gluon field evaluated over the weak coupling region is essentially *common* to all events with different hadronic final states raises a very interesting possiblilty. It suggests that the *Event Weight Functions* for all the final states can be evaluated by the expectation value of a fermion loop along the classical path in strong coupling which involves only the area of world surface determined by the fermion loop. According to this picture, events with hadrons which

have big P_T's will be suppressed since the events have large world surface area and will be suppressed by $e^{-b'\mathcal{A}}$. Thus, the picture is qualitatively capable of explaining the fact that jetty events are preferred to non-jetty events and 2-jet events are preferred to 3- or more jet events. In the future development of the UCLA model (UCLA 'stage 3'), it will be attempted to construct the *Event Weight Function* for a given final state from such a *warped area-law* approach, which subsumes the parton shower treatment into the area-law approach, and to simulate whole events at a time rather than an iterative implementation.

7 Summary and Future Work

The hadronization process is a very interesting challenge from a QCD viewpoint in that (a) it is a fundamental QCD process, (b) it can be studied experimentally extensively in a detailed clean fashion in e^+e^- interactions and with particularly simple fundamental probes in the form of flavored meson rates and distributions, and (c) it is a transition, as the initial quark and antiquark rapidly separate, from an original high-virtuality state where perturbative calculations can be performed to a very soft low-virtuality non-perturbative regime, traditionally the domain of lattice work and strong-coupling expansion calculations.

We have shown and discussed the steps in an emerging conceptual and calculational path from QCD to successful predictions of e^+e^- annihilation rates and distributions into hadrons (the simplest arena in which to study quark-colorfield behavior). Central to this path is construction of an *Event Weight Function* which, for our stringent UCLA assumptions, depends only on a QCD-motivated space-time area law, approximate longitudinal phas-espace, and factors to knit quarks into hadronic wave functions (Clebsch-Gordon coefficients for flavor and spin, and a universal *'knitting'* factor for spatial wave functions).

Our approach is particularly successful in predicting data on light-quark meson production, thereby contributing to our understanding of this simplest manifestation of colorfield behavior. It also forms a foundation for further understanding of more sophisticated colorfield behavior – e.g., baryon formation, P_T effects, spin-spin correlations, etc – as larger samples of more detailed data become available in the future.

The *Event Weight Function* – a simple phenomenological model – also performs the valuable role of a *'target'* for physicists interested in various QCD theoretic approaches to hadronization – e.g., Euclidean-space lattice work, relativistic string modeling, approximate Minkowski-space calculations using new emerging techniques such as world-line formalism – to use as possible verification of their work.

Work to be done in the future includes:

(1) Accumulation of large flavor-identified data samples such that accurate two- and three-particle distributions can be studied in order to understand baryon formation, P_T effects, spin-spin correlations, etc. on the same level as the present understanding of meson formation.

(2) More highly developed phenomenological Monte Carlo modeling, in particular of phenomena such as popcorn production and local P_T compensation, in order to help interpret the data on these phenomena.

(3) Continued lattice work to understand the shape and possible decay of the colorfield between a quark and antiquark.

(4) As QCD calculational techniques continue to improve, attempts to derive the Event Weight Function structure (or modifications of it) and then to predict the parameter values within this structure, in particular (a) the vertex suppression factors, which our UCLA model assumes are all approximately 1.0 for $u\bar{u}$, $d\bar{d}$, $s\bar{s}$ and 0.0 for $c\bar{c}$ and $b\bar{b}$, and (b) the knitting factors, which UCLA assumes are all approximately equal and for which probability unitarity of the *integrated/summed* fragmentation function leads to a value around $1/(75MeV)^{-2} \simeq (2.7fm)^2$.

(5) Attempts to calculate and/or understand, either from a QCD-basis or from other physical mechanisms, the values of the 'natural' constants 'a' and 'b'; e.g., using spin-and-spectator-quark counting arguments from deep inelastic crossing symmetry to estimate 'a' values for mesons and baryons.

(6) Attempts to develop the 'Initial-to-Final-State Global' approach (UCLA 'stage 3') described in Section 6 in which the parton shower is treated as an unobserved intermediate state and an area law type of approach

is applied to the entire transverse momentum (combining P_T from gluons and P_T from the finite colorfield width) of a set of specified final state hadrons.

For those interested in working with our model, the program and manual can be found at *www.physics.ucla.edu/∼chuns.*

Acknowledgement We are deeply indebted to members of the Lund group - Bo Andersson, Hans-Uno Bengtsson, Gösta Gustafson, Gunnar Ingleman, Torbjörn Sjöstrand - for many important and illuminating conversations in the development of this ansatz. We gratefully acknowledge stimulating and useful discussions with Zwi Bern, Siegfried Bethke, Dick Blankenbecler, Stan Brodsky, Phil Burrows, Mike Cornwall, Brent Corbin, Glen Cowan, Alessandro deAngelis, Eric D'Hoker, Tom Gottschalk, Werner Hofmann, J.K.Kim, Duncan Morris, Roberto Pecci, Ina Sarcevic, Terry Tomboulis, Douglas Toussaint and Brian Webber. We especially want to thank Rick Berg (who compiled the 'world average' data used at 10 GeV and 29 GeV), Sahak Khacheryan (who suggested the heavy quark modification leading to $z_{\rm eff}$), James Yentang Oyang (who participated extensively in several phases of the work), and Hiroaki Yamamoto (who presented many illuminating challenges to the ansatz).

References

[1] C.D. Buchanan and S.-B. Chun, Phys. Rev. Lett. 59 (1987) 1997

[2] B. Anderson *et al.*, Z. Phys. **C**20 (1983) 317

[3] B. Anderson *et al.*, Phys. Rep. 97 (1983) 33

[4] S.-B. Chun and C.D. Buchanan, Phys. Lett. **B**308 (1993) 153

[5] K. Wilson, Phys. Rev. **D**10 (1974) 2445

[6] T. Sjöstrand, Comp. Phys. Comm. 82 (1994) 74

[7] This solution was first implicitly used by the Lund group in reference [2] where they showed that the assumption of $g(S) \propto S^a$ for large S

connected the area law with the Lund Symmetric Fragmentation Function, which they had derived from a left right symmetry requirement. A rigorous proof can be found in the reference [17].

[8] Private communication from Gösta Gustafson, Lund.

[9] J.M. Cornwall, UCLA/96/TEP/15 (unpublished)

[10] E.C. Berg and C.D. Buchanan, UCLA-HEP-95-01 (Unpublished)

[11] A. De Angelis, CERN-PPE/95-135

[12] XXVIII International Conference on High Energy Physics, July, 1996, Warsaw, Poland

[13] C. Peterson, *et al.*, Phys. Rev. **D** 27 (1983) 105

[14] P.D.Acton, *et al.*, Phys. Lett. **B** 305 (1993) 415

[15] G.S. Bali, K. Schilling, Ch. Schichter, CERN-TH 7413/94;
The UK QCD Collaboration, Phys. Lett. **B**275 (1992) 424;
R.W. Haymaker, et al, LSUHE 94-159;
Y. Peng and R.W. Haymaker, Nucl. Phys. **B**34 (1994) 266

[16] W. Feilmair and H. Markum, Nucl. Phys. **B**370 (1992) 299

[17] Sebong Chun and Charles Buchanan, 'A Simple Plausible Path from QCD to Successful Prediction of $e^+e^- \rightarrow$ *Hadronization* Data', accepted for publication by Physics Reports. UCLA-HEP-97-01

[18] K. Wilson, Phys. Rep. 23 (1975) 331